In presenting the dissertation as a partial fulfillment of the requirements for an advanced degree from the Georgia Institute of Technology, I agree that the Library of the Institute shall make it available for inspection and circulation in accordance with its regulations governing materials of this type. I agree that permission to copy from, or to publish from, this dissertation may be granted by the professor under whose direction it was written, or, in his absence, by the Dean of the Graduate Division when such copying or publication is solely for scholarly purposes and does not involve potential financial gain. It is understood that any copying from, or publication of, this dissertation which involves potential financial gain will not be allowed without written permission.

_____

_____

3/17/65
b

A MOLECULAR RESONANCE AUTOMATIC FREQUENCY CONTROL SYSTEM FOR MILLIMETER OSCILLATORS

A THESIS

Presented to

The Faculty of the Graduate Division

by

Milton Edward Cram

In Partial Fulfillment

of the Requirements for the Degree

Doctor of Philosophy

in the School of Electrical Engineering

Georgia Institute of Technology

September, 1967

A MOLECULAR RESONANCE AUTOMATIC FREQUENCY

CONTROL SYSTEM FOR MILLIMETER OSCILLATORS

Approved:

Chairman

Date approved by Chairman: 10-24-67

ACKNOWLEDGMENTS

The author is grateful to Dr. D. T. Paris for his patience, guidance, and advice during this investigation. The valuable discussions, guidance and support of Dr. F. K. Hurd and Dr. D. C. Ray will always be remembered and appreciated.

I also express appreciation to Dr. A. P. Sheppard and Dr. J. Q. Williams for technical guidance during the early part of this investigation, to the Engineering Experiment Station Machine Shop for assistance in constructing the waveguide absorption cell, and to the many others who have worked to make the completion of my graduate studies possible.

My deepest appreciation goes to my wife, Linda, and three children, Marc, Brian, and Lorie, for their continuous patience, understanding, and encouragement.

TABLE OF CONTENTS

APPENDICES (Continued) Page

LIST OF ILLUSTRATIONS

SUMMARY

The rapid decrease in available frequencies in the longer wavelength portion of the electromagnetic spectrum has stimulated interest in the millimeter and submillimeter regions. Of primary concern in these regions is the problem of oscillator frequency stability and the selection of suitable references for control systems.

The existence of numerous molecular resonance absorption lines throughout the millimeter portion of the spectrum has been demonstrated by the microwave spectroscopists. Moreover, they have shown that each line possesses a spectral shape that is accurately predicted by the theory of Van Vleck and Weisskopf. In addition, the microwave spectroscopists have shown that individual absorption lines may be shifted under the influence of a perturbing electric field. This effect is known as the Stark effect.

This investigation was undertaken to determine the feasibility of using Stark shifted molecular absorption lines as oscillator AFC references. Utilizing known molecular characteristics a molecular resonance frequency discriminator was predicted.

An oscillator AFC system, based on the $J = 1 \rightarrow 2$ transition of methyl fluoride, CH_3F, was constructed and evaluated at Georgia Tech under NASA Institutional Grant NsG-657. The system consists of a 98-104 GHz reflex klystron, a waveguide absorption cell, a Stark modulation source, a crystal detector, a tuned amplifier, a synchronous demodulator, a low-pass amplifier, and various power supplies.

Application of an 11 kHz alternating Stark field to an electrode within the specially constructed waveguide absorption cell provided modulation of the amplitude of a wave transmitted through the cell. This modulation was effected by periodic variations in the natural molecular resonance frequency and thus contained information regarding the mean separation of the oscillator and molecular resonance frequencies.

The crystal detector, tuned amplifier, and synchronous demodulator were used to develop a control voltage based on the modulation of the absorption cell output produced by the Stark field. This voltage was then employed, in a feed-back system, to control the frequency of the klystron.

Utilizing observed molecular characteristics and the characteristics of the microwave components and electronic circuitry, a closed loop gain of approximately 1200 was predicted. Laboratory tests indicated that an actual closed-loop gain in excess of 900 was obtained. Thus fair agreement of the observed and calculated gains was achieved.

In addition, an open-loop drift of about one part in 10^5 per hour was measured for the klystron selected. Closed-loop data indicate that a stability of approximately one part in 10^7 per hour was achieved with the methyl fluoride AFC system. Due to the presence of noise, however, the short-term stability was limited to about three parts in 10^7 for time intervals much less than one second.

The long-term stability of the system compares favorably with that of crystal oscillator referenced phase-lock techniques used at

lower frequencies. The observed stability, however, was limited somewhat by the quality of the crystal detector and dc Stark field source. The technique reported here appears to be reliable, and should be applicable at other frequencies. Furthermore, recent advancements in the development of new detectors indicate that additional improvement is possible.

CHAPTER I

INTRODUCTION

Technical developments during the last quarter of a century have made systems operating at frequencies up to the order of 25 GHz commonplace. With the advent of new signal sources capable of generating usable quantities of microwave power at higher frequencies, considerable interest in the utilization of the spectrum above 25 GHz has arisen. Communications systems, precision radars, and telemetry systems are rapidly being developed to meet the needs of industry and government for wider system bandwidths, thereby creating greater information handling capacity. As these systems are placed in operation, the unoccupied portion of the spectrum decreases, providing further impetus to examine the spectrum between 25 GHz and optical frequencies. Furthermore, the higher frequencies provide certain inherent advantages. Components may be made smaller than corresponding elements at lower frequencies. Also, complicated mathematical analysis may frequently be replaced by simpler optical analysis. For example, ray tracing may be used in the design of such elements as antennas.

The existence of several maxima and minima in atmospheric absorption throughout the millimeter portion of the spectrum may be a problem when long atmospheric paths are involved. The judicious selection of operating frequencies, however, can usually provide satisfactory performance. A more serious problem is that of oscillator frequency

stability. Certain laboratory systems, such as microwave spectroscopes, and various types of communications systems require a high degree of frequency stability. In situations where the inherent stability of the oscillators involved is unsatisfactory, an automatic frequency control system must be employed.

Essential to the operation of any automatic control system is a method for obtaining an error signal which is proportional to the difference between the frequency of the source and a reference. In general, there are three types of stabilization systems. The first type may be identified by the use of a reference frequency much greater than the operating frequency. The second type employs a reference which is much lower in frequency than the desired operating frequency while the third system utilizes a reference at, or near, the desired frequency of operation. In each case, the reference must be compared with the oscillator to be stabilized so that a control signal may be developed.

The two most common methods for obtaining the control signal are based on either a static comparison of reference and source frequencies, which is usually impractical at millimeter wavelengths, or a comparison of a frequency modulated source with a fixed reference. A third alternative, although very uncommon, employs a fixed source and a frequency modulated reference. This latter method may be beneficial if the mean frequency of the reference retains its stability while the instantaneous frequency is modulated. Moreover, modulation of the reference allows the desirable condition of stabilizing an unmodulated oscillator.

At the lower microwave frequencies, stabilization systems employing references at the operating frequency, or much lower than the

operating frequency, are very common. For example, radar transmitters are often stabilized by comparison of the source frequency with a resonant metallic cavity or a harmonic of a low frequency crystal oscillator. The ammonia, cesium, hydrogen, and rubidium clocks, on the other hand, are representative of systems of the third type. That is, these devices employ an atomic resonance, occurring at a microwave frequency, to stabilize crystal oscillators at frequencies of a few MHz.

Obviously, systems of the first type (reference frequency much greater than the operating frequency) are not feasible at millimeter wavelengths since references at yet higher frequencies would be extremely difficult to obtain. As an alternative, the second type of stabilization, employing a low frequency reference, may be used. However, a large amount of equipment is usually required. Also, the fabrication and maintenance problems often are prohibitive.

Resonant devices such as the Fabry-Perot interferometer may be utilized for the third type of stabilization. To achieve long term stability some form of temperature compensation must be employed. In addition to the complex temperature regulation equipment, difficulties in maintaining mechanical tolerances in fabrication may present severe limitations.

In contrast to man-made resonant devices for stabilization at, or near, the reference frequency are molecular resonances. Examination of the literature reveals a large number of observed molecular rotational resonances throughout the millimeter wavelength portion of the spectrum. These resonances, as they are normally applied in frequency control systems, exhibit themselves as extremely stable narrow-band

absorption regions. In fact, since the spectral widths of these regions are often small compared to the center frequencies, the term *line* is commonly used when referring to each narrow region of absorption.

Existing techniques employing molecular resonances rely on the inherent stability of stationary absorption lines and obtain a control signal by sampling the resonance through modulation of the source frequency. Microwave spectroscopists, however, have shown that the application of a controlled electric field may produce calculable shifts in the resonant frequencies of particular molecules. This effect, known as the *Stark effect*, thus presents itself as a logical candidate for a stabilization system of the third type, utilizing modulation of the reference frequency.

This investigation was undertaken to determine the feasibility of using Stark-shifted molecular rotational resonance lines for stabilization of a millimeter wavelength reflex klystron oscillator. The objective was to show that application of microwave spectroscopy techniques may produce a new type of frequency discriminator which is both simple and inexpensive. On the basis of known molecular parameters, the molecular discriminator, when employed in a feed-back loop, is shown to be theoretically capable of providing a significant improvement in oscillator frequency stability.

To demonstrate the validity of the calculations and the simplicity of the method, an experimental system based on the $J = 1 \rightarrow 2$ rotational transition of methyl fluoride, CH_3F, at approximately 102 GHz, was constructed. Utilizing a waveguide absorption cell filled with the molecular gas at a pressure of about 0.1 mmHg and a Stark modulation system,

the predicted discriminator action of a moveable absorption line was verified and evaluated.

A discussion of the molecular resonance theory essential to an understanding of the molecular frequency discriminator is presented in Chapter II. Chapter III describes the mathematical model of the system. Chapter IV contains a discussion of measurement techniques required for a determination of various parameters in the mathematical model. Chapter V describes the experimental stabilization system used to verify and evaluate the molecular resonance frequency discriminator. Chapter VI presents conclusions resulting from this investigation and recommendations for future work. The Appendices contain additional information on resonant frequencies, line shapes, the Stark effect, and a method for predicting the loss due to the material supporting the Stark electrode within the absorption cell.

CHAPTER II

A MOLECULAR RESONANCE FREQUENCY DISCRIMINATOR

The historic experiments of Cleeton and Williams (1) in 1934 first demonstrated the absorption of microwave energy by ammonia molecules. More recently, microwave spectroscopists have shown that numerous other molecules, each possessing a permanent electric or magnetic dipole moment, also exhibit absorption in one or more regions of the spectrum. This absorption of microwave energy is manifested through a reduction in the amplitude of electromagnetic waves of particular frequencies as the waves propagate through space containing the dipolar molecules. At low pressures, and hence low molecular densities, the frequencies of the electromagnetic waves for which appreciable absorption is observed are found to lie in relatively narrow regions scattered throughout the microwave spectrum. Although the regions of absorption are finite in spectral width, they often appear as discrete lines when a wide spectral region, showing one or more peaks of absorption, is presented graphically. Hence, the term *line* is commonly used when referring to each narrow region of absorption. Upon close inspection, though, the lines are shaped, as a function of frequency, much the same as the impedance plot of an RLC network in the vicinity of a resonance.

Further investigations by the microwave spectroscopists revealed that the application of a static, or slowly varying, electric field, to

a region of *molecules having permanent electric dipole moments*, may produce observable shifts in the frequencies at which maximum absorption occurs. In addition, lines that appear as a single line in the absence of the applied field may spread apart when the field is applied, thereby forming more than one line. This effect is known as the Stark effect. In the case of molecules possessing permanent magnetic dipole moments, a magnetic analog known as the Zeeman effect is observed when a static or slowly varying magnetic field is applied.

In the following sections, a review of the pertinent theory of molecular resonances, linewidths, and the Stark effect will be presented. The significant aspects of the theory will be tied together to demonstrate the possibility of molecular resonance frequency discriminators. Such devices, possessing the inherent stability of a molecular system, have obvious applications in the field of automatic frequency control of millimeter oscillators.

Molecular Resonance

To explain the phenomena observed by the microwave spectroscopists, one might consider the molecule as a small rotating dipole. If classical methods are used, however, no explanation of the discreteness of the observed absorption lines will be provided. Quantum mechanical models, on the other hand, predict that only certain, discrete values of total molecular energy are allowed. The various components of the total energy, such as electronic, nuclear, vibrational, and rotational energies, are also allowed only discrete values. Furthermore, a quantum of energy, ε_{ij}, equal to the difference in total energies of two allowed states i

and j, must be absorbed or emitted when a transition between these two states occurs. Also, wave-particle duality requires that a frequency f_{ij} be associated with each quantum according to Planck's law, $\varepsilon_{ij} = hf_{ij}$, where h is Planck's constant. Hence, a molecular system may absorb energy from an electromagnetic wave if the frequency of the wave is such that the energy of the individual quanta corresponds exactly to the energy difference between two allowed states and provided that the upper level is not already completely filled.

In the microwave region the primary source of absorption has been shown to be produced by transitions between rotational energy states. Thus a knowledge of the allowed rotational energies is required for an accurate prediction of absorption frequencies. A method for calculating the discrete, or quantized, energy levels of a rigid rotating molecule is described in an early paper by Reiche and Rademacher (2). In particular, the wave functions, or equations of motion, for symmetric-top molecules* are discussed. Utilizing an operator method suggested by Schrödinger (3), a wave equation is formulated and solved, thereby yielding wave functions that describe all allowed rotational states of the molecule. A review of the procedures of Reiche and Rademacher is presented in Appendix A.

A significant conclusion from the aforementioned work is that each particular allowed rotational state may be completely characterized by

---

*Symmetric top molecules are molecules possessing an axis of at least three-fold rotational symmetry and with equal moments of inertia about two axes, each orthogonal to the symmetry axis and to each other.

three integers, called quantum numbers. These numbers are commonly denoted J, K, and M. As shown in Appendix A, they may be associated with various components of the molecule's angular momentum and satisfy the relationships $|K| \leq J$ and $|M| \leq J$. Consequently, a particular energy state may be designated $\varepsilon(J,K,M)$ and the expression for the absorption frequency, f_o, corresponding to a transition from an energy state $\varepsilon(J_1,K_1,M_1)$ to another state $\varepsilon(J_2,K_2,M_2)$ may be written as

$$f_o = \frac{\varepsilon(J_2,K_2,M_2) - \varepsilon(J_1,K_1,M_1)}{h} \qquad (2\text{-}1)$$

For absorption to occur, the frequency of an incident electromagnetic wave must equal the natural molecular frequency, f_o, predicted by (2-1). Hence, f_o is commonly called the *molecular resonance frequency.*

A further consequence of the quantum theory is that transitions between any two arbitrary states may not necessarily be allowed. Since the wave functions are actually probability functions, certain transitions may have a zero probability of occurrence. In the case of a symmetric-top molecule, it has been shown that the following conditions, or selection rules, must be obeyed for a nonzero rotational transition probability to exist:

$$J_2 = J_1 \pm 1, \quad K_2 = K_1, \quad \text{and} \quad M_2 = M_1$$

Thus, as shown in Appendix A, Equation (2-1) may be recast in the

form (see Equation (A-14))

$$f_o = 2B(J + 1) \tag{2-2}$$

where B is a molecular constant.

Contrary to the assumed conditions, experimental evidence indicates that the molecules are not perfectly rigid, and may, therefore, be deformed by vibrations or centrifugal forces. Generally, however, the effects of vibrations and centrifugal distortion are small and may be treated as perturbations. Nielson (4) presents general expressions to account for centrifugal distortion in certain symmetric-top molecules. He concludes that stretching of the molecule due to centrifugal forces increases the molecular moment of inertia, thereby altering the rotational energy and, hence, the observed transition frequencies. Furthermore, a study of the effect of vibrations by Gordy et al. (5), led to the conclusion that vibrations introduce negligible splitting of the transition frequencies for most symmetric-top molecules. However, as in the case of centrifugal distortion, the effective moment of inertia may be altered by vibrations. To compensate for these effects, Equation (2-2) is commonly written in the form

$$f_o = 2(B_e - D_{JK}K^2)(J + 1) - 4D_J(J + 1)^3 \tag{2-3}$$

where the constants D_J and D_{JK} account for centrifugal distortion. In addition, the constant B of (2-2) has been replaced by B_e to include vibrational effects. In succeeding sections, the molecular resonance

frequency will be assumed to be given by (2-3), unless perturbing fields are known to be present. In such cases, appropriate modifying terms, to be discussed later, must be added to (2-3).

Line Widths

The variation of the observed linewidths with a reduction in pressure has led various analysts to examine the theoretical effect of molecular collisions on the linewidths. The most widely accepted theory is that of Van Vleck and Weisskopf (6). A review of their work, reproduced in Appendix B, reveals that the fraction, α, of the energy absorbed from a plane electromagnetic wave per unit of thickness traversed may be represented in the frequency domain by an expression of the form.

$$\alpha = \alpha_o \left[\frac{(\Delta f)^2}{(f - f_o)^2 + (\Delta f)^2} + \frac{(\Delta f)^2}{(f + f_o)^2 + (\Delta f)^2} \right] \qquad (2\text{-}4)$$

where α_o is a constant, f_o is the molecular resonance frequency, and Δf, the line width parameter, is equal to $(2\pi)^{-1}$ times the reciprocal of the mean time between collisions.

Since the mean time between collisions is proportional to the reciprocal of the density and, hence, pressure, Δf is linearly proportional to pressure (7). Thus, the operating pressure may be reduced sufficiently so that Δf is much smaller than f_o. The second term within the brackets of (2-4) may then be neglected, in which case,

$$\alpha \approx \alpha_o \frac{(\Delta f)^2}{(f - f_o)^2 + (\Delta f)^2} \qquad (2\text{-}5)$$

Hence, for the low pressures commonly used in microwave spectroscopy, a maximum attenuation α_o is observed at the frequency $f = f_o$. Moreover, Δf is evidently the half-line width at half maximum absorption (i.e., when $\alpha = \frac{\alpha_o}{2}$).

In the event that the second term in (2-4) may not be neglected, the frequency at which maximum α is observed may be found by differentiating the right-hand member of (2-4) with respect to f. Setting this derivative equal to zero yields an expression for the frequency of maximum absorption. Following this procedure, the desired frequency is $f_o\left[1 + \left(\frac{\Delta f}{f_o}\right)^2\right]$. Thus, the deviation of the frequency of maximum absorption from that observed at very low pressures (where $\Delta f << f_o$) is second order in Δf and may be neglected for sufficiently small Δf.

An additional factor that must be dealt with at extremely low pressures is the effect of random molecular velocities. Because of thermally induced linear motion, each molecule "sees" a Doppler shift in the frequency of an incident electromagnetic wave. On the basis of the commonly assumed Boltzmann distribution of molecular velocities, the predicted line shape is Gaussian and has a half-line width at half maximum absorption given by

$$\Delta f_{\text{Doppler}} = \frac{f_o}{c} \sqrt{2kN_o \ell n 2} \sqrt{\frac{T}{M}}$$

where c is the velocity of light, k is Boltzmann's constant, N_o is

Avogadro's number, T is the absolute temperature of the molecular gas, and M is the molecular weight (8).

With the exception of very low pressures, the line width parameter Δf is determined primarily by collision effects. However, at pressures where the effect of Doppler broadening must be included, Townes and Schawlow (9) show that the total line width parameter is given very nearly by

$$\Delta f \approx \left[(\Delta f_{\text{Doppler}})^2 + (\Delta f_{\text{Collisions}})^2 \right]^{\frac{1}{2}}$$

For pressures greater than several hundredths of a millimeter of mercury, $\Delta f_{\text{collision}}$ dominates, the Van Vleck-Weisskopf theory applies, and a linear variation of Δf with pressure is predicted.

The Stark Effect

As noted previously, the application of an electric field to a molecule possessing a permanent electric dipole moment alters the transition frequencies. Thus, it may be assumed that the observed line is centered at a frequency f_o' given by

$$f_o' = f_o + a_1 E + a_2 E^2 + \cdots \qquad (2\text{-}6)$$

where f_o is the line center in the absence of the applied electric field intensity, E, and where the coefficients a_1, a_2, etc., relate the observed frequency shift to the applied field. In most cases of interest it has been experimentally demonstrated that the total shift, $f_o' - f_o$,

is small relative to the transition frequency, f_o. Hence, f_o may be calculated according to Equation (2-3) and the coefficients a_1, a_2, etc., evaluated by means of quantum mechanical perturbation techniques. A general method by which these coefficients may be calculated is discussed in Appendix C.

Assuming that the applied electric field is parallel to the electric field vector of the electromagnetic wave, the first two coefficients, a_1 and a_2, are shown in reference (10) to have the form

$$a_1 = \frac{\mu\ 2MK}{J(J+1)(J+2)h} \tag{2-7a}$$

$$a_2 = \frac{\mu^2}{(J+1)Bh^2}\ \frac{3M^2(8J^2+16J+5) - 4J(J+1)^2(J+2)}{J(J+2)(2J-1)(2J+1)(2J+3)(2J+5)} \tag{2-7b}$$

where μ is the permanent electric dipole moment and the remaining symbols are as defined earlier. Additional coefficients could be calculated as needed.

In the case of symmetric-top molecules with $K \neq 0$, it may be shown that the contribution of the term a_2E^2 and higher order terms in (2-6) may be neglected with respect to a_1E for values of E less than several tens of volts per centimeter. Thus, the shift in the center frequency of the absorption line is essentially a linear function of E. The appropriate expression for the center frequency of a Stark shifted absorption line of a symmetric top molecule is, therefore,

$$f_o' = f_o + \frac{(\mu E)2MK}{J(J+1)(J+2)h} \qquad (2\text{-}8)$$

As noted earlier, M and K are each integers and satisfy the relations $|M| \leq J$ and $|K| \leq J$. Consequently, lines which correspond to K values of equal magnitude but opposite sign and which coincide in the absence of an applied E now shift in opposite directions. Moreover, the shifted frequencies are dependent upon M when a field is applied. Further discussion of these effects will be presented later.

For linear molecules, which have a very small moment of inertia about the molecular axis, the energy associated with rotation about that axis is extremely large. Thus, it is highly improbable that a linear molecule will be in a state possessing angular momentum about the molecular axis as a result of thermal energy. Furthermore, the energy associated with the quanta of microwave signals is also insufficient to excite such states. As a consequence, the quantum number K, as defined in Appendix A, may be assumed to be identically zero for linear molecules. The coefficient a_1 is, therefore, also zero and the dominant coefficient is found to be a_2. Hence, the center frequency of a Stark shifted absorption line of a linear molecule is given by

$$f_o' = f_o + \frac{(\mu E)^2}{(J+2)Bh^2} \frac{3M^2(8J^2+16J+5) - 4J(J+1)^2(J+2)}{J(J+2)(2J-1)(2J+1)(2J+3)(2J+5)} \qquad (2\text{-}9)$$

A Molecular Frequency Discriminator

Examination of Equation (2-4) reveals that the magnitude of an electromagnetic wave passing through a region containing dipolar molecules may be modulated simply by varying either the molecular resonant frequency, f_o, or the frequency, f, of the incident wave. Hence, one may consider the line shape as a transfer function relating frequency changes to variations in the amplitude of the wave. Since f and f_o occur only in the term $(f - f_o)^2$, either one may be considered as the variable while the remaining one is assumed constant. For sinusoidally varying f, f_o being fixed, the variations in the wave amplitude may be determined from Figure 1. From this figure, it is evident that the amplitude modulation of the wave is dependent upon both the maximum change in f and the relative separation of the line center and the mean frequency of the wave. Thus, for frequencies far removed from the line center, in either direction, little or no amplitude modulation is detected. When the mean frequency of the wave is below the line center, but within a few linewidths, the wave amplitude is shown to be nearly sinusoidal and with the same period as the modulation frequency. However, the wave amplitude decreases for increasing wave frequencies resulting in a 180° phase relationship between the modulating signal and the wave amplitude. When the mean frequency of the wave in coincident with the line center, it is evident that both positive and negative excursions of the wave frequency yield an increase in the wave amplitude. Hence, the wave amplitude is shown to vary periodically at twice the frequency modulation rate. Finally, for a mean wave frequency greater than the line center frequency, but within a few linewidths, Figure 1 shows that the

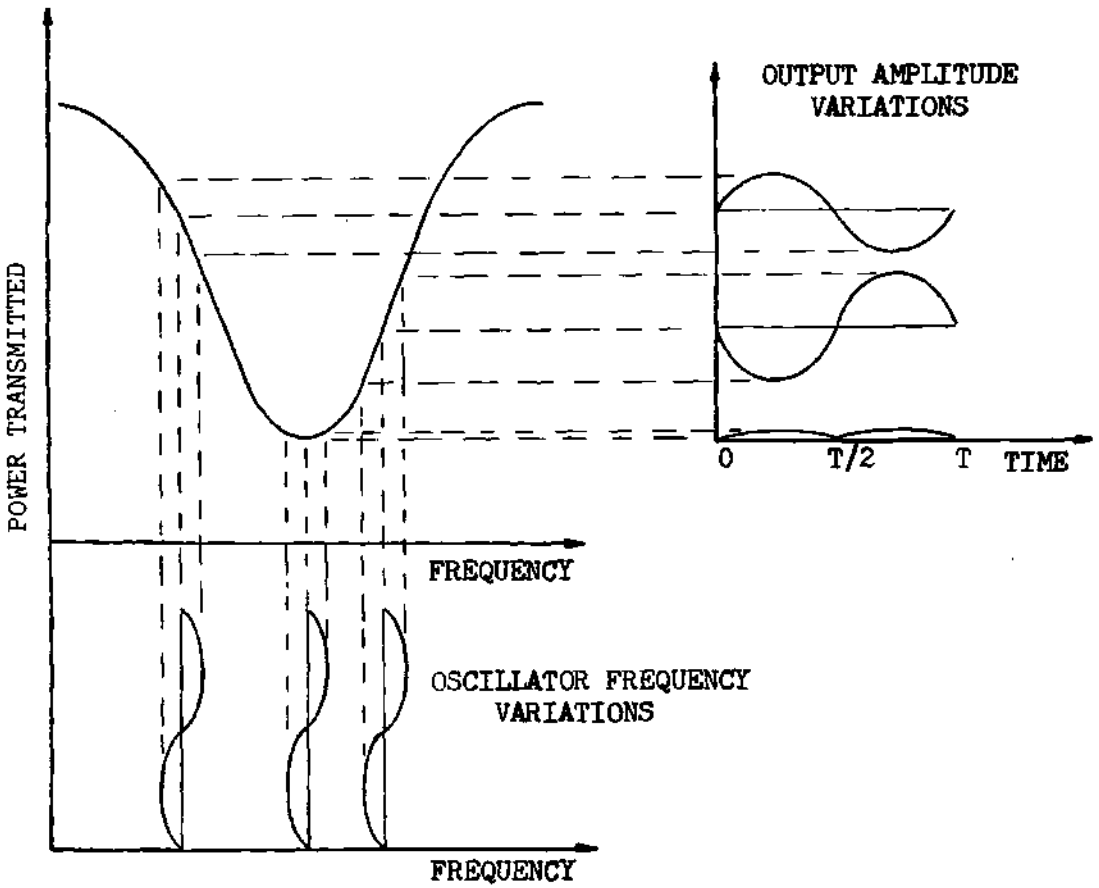

Figure 1. Absorption Cell Output Variations due to Oscillator Frequency Modulation

amplitude modulation is nearly sinusoidally and in phase with the frequency modulation. It should be evident, therefore, that the component of the wave amplitude which varies at the modulation rate* exhibits the typical S-curve discriminator function when plotted versus the separation between the mean wave frequency and the line center.

A stabilization scheme utilizing this type of discriminator is described by Fletcher and Cook (11) and is shown in Figure 2. A sealed section of waveguide, filled with a molecular gas at a suitable pressure, and terminated with a detector, is used to convert the wave frequency variations to voltage variations which are proportional to the modulation of the wave amplitude. A phase sensitive device is then used to compare the amplitude and phase of the detector output with the signal used to modulate the wave frequency. A control voltage is thereby derived which allows the mean frequency of the wave to be forced toward the line center. Although simple in concept and design, this system possesses the inherent disadvantage of having an output which is frequency modulated.

An alternative to modulating the frequency of the gas, or the frequency of the oscillator to be stabilized, was proposed by Herschberger and Norton (12). Their system, as illustrated in Figure 3, requires a separate oscillator for examining the molecular resonance. A comparison of the envelope of the intermediate-frequency amplifier output with the amplified absorption cell detector voltage provides

---

*It is assumed that a negative sign may be used to denote 180° phase reversals.

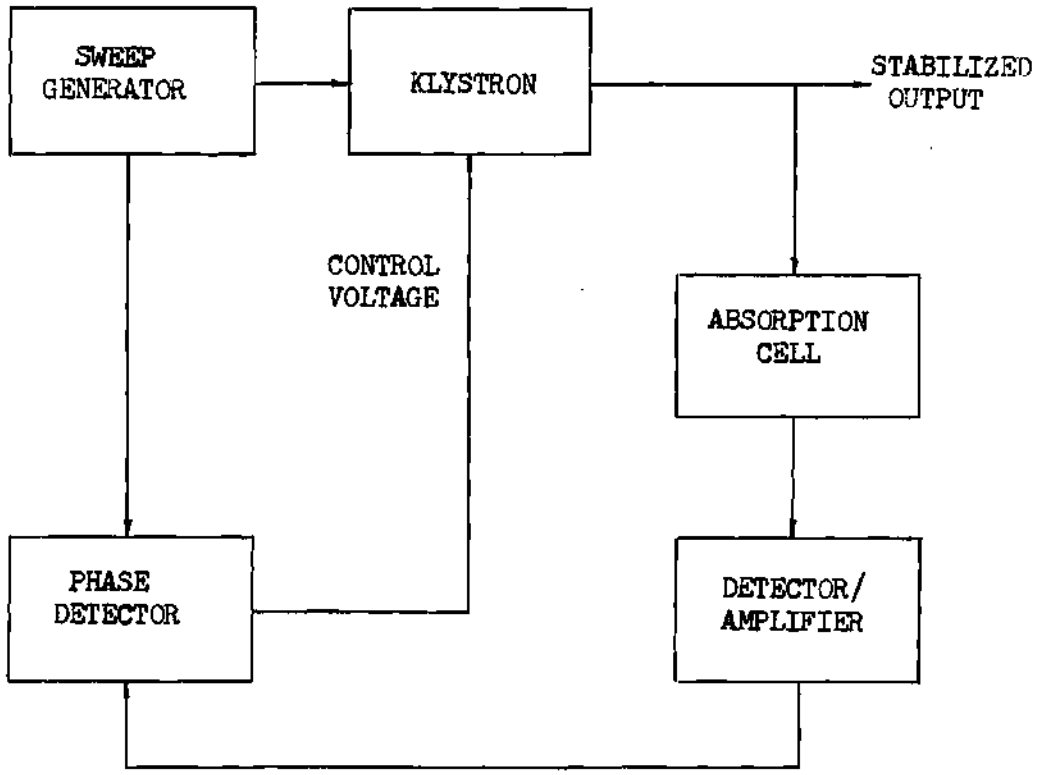

Figure 2. A Molecular Resonance AFC System-After Fletcher and Cooke (11)

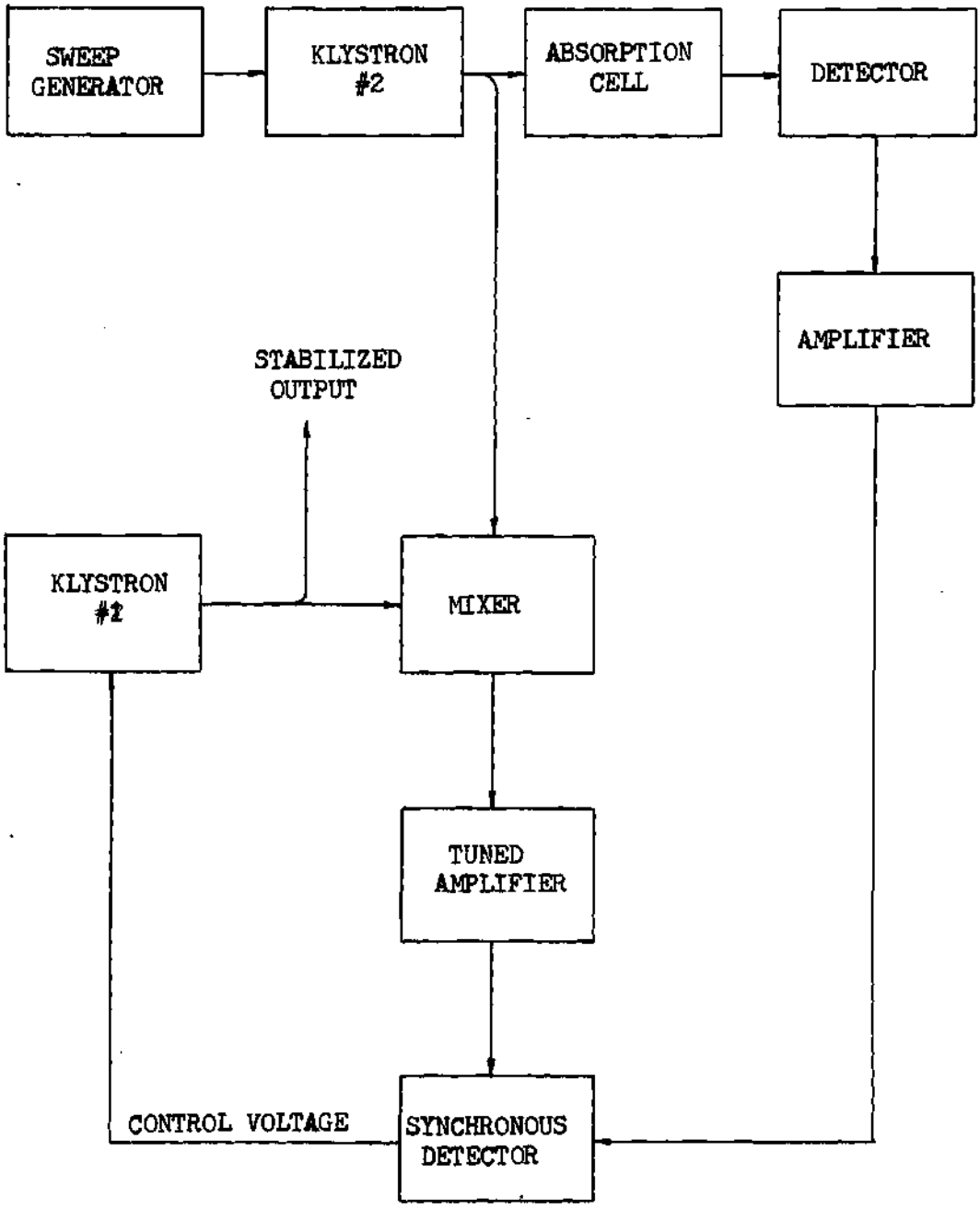

Figure 3. A Molecular Resonance AFC System-After Hershberger and Norton (12)

the necessary stabilizing voltage. This method of stabilization is based on the following facts:

1. If the beat between the sweep oscillator and the stabilized oscillator is centered in the pass-band of the intermediate-frequency amplifier at the same instant the sweep oscillator frequency passes through maximum absorption, the output of the coincidence detector is zero.

2. Whenever the maximum of the intermediate-frequency amplifier output and the absorption cell detector output occur at different times, a correction voltage is developed whose polarity depends upon which signal occurs first. Although the system allows stabilization at a frequency different from the molecular resonance by selection of the center frequency of the intermediate-frequency amplifier, the cost of the additional oscillator and power supply may be prohibitive. Moreover, some sacrifice in stability may result due to variations in the amplifier center frequency.

A simple and inexpensive alternative to the above methods, is found in an application of the previously described Stark effect.

Shifting the molecular resonance frequencies enables the wave amplitude to be modulated while the wave frequency is held fixed. Thus, f_o in (2-5) may be assumed to be of the form (for a symmetric-top molecule)

$$f_o = f + \delta f + a_1(E_1 + E_2 \sin\omega_m t) \qquad (2\text{-}10)$$

where f is the frequency of the oscillator to be stabilized, δf is the

separation between the oscillator frequency and the line center when the Stark field is zero, a_1 is the Stark shift coefficient given by (2-7a), E_1 and E_2 are the dc and alternating components of the Stark voltage, respectively, and $\omega_m/2\pi$ is the modulation frequency.

From (2-10), the difference $(f - f_o)$ may be formed and inserted into (2-5) to give

$$\alpha(t) = \alpha_o\left[\frac{(\Delta f)^2}{(\delta f + \beta \sin\omega_m t)^2 + (\Delta f)^2}\right] \tag{2-11}$$

where E_1 is assumed zero and a_1E_2 is replaced by β.

The above closed-form expression may also be represented as a Fourier series:

$$\alpha(t) = \alpha_o\left[d_o + \sum_{i=1}^{\infty} c_i \sin i\omega_m t + d_i \cos i\omega_m t\right] \tag{2-12}$$

If it is assumed that any variations in f are slow compared to $\omega_m/2\pi$, δf may be considered as a constant. Hence, the coefficients c_i and d_i may be calculated by standard Fourier techniques. Thus c_1 is obtained by equating the right-hand members of (2-11) and (2-12), multiplying by $\sin\omega_m t$, and integrating from $t = -\frac{\pi}{\omega_m}$ to $t = +\frac{\pi}{\omega_m}$:

$$c_1 = \frac{\int_{-\pi/\omega_m}^{\pi/\omega_m} \frac{(\Delta f)^2 \sin\omega_m t\,dt}{(\delta f + \beta\sin\omega_m t)^2 + (\Delta f)^2}}{\int_{-\pi/\omega_m}^{\pi/\omega_m} \sin^2\omega_m t\,dt} \qquad (2\text{-}13)$$

The coefficient d_1 is obtained in a similar manner except that $\sin\omega_m t$ is replaced by $\cos\omega_m t$.

$$d_1 = \frac{\int_{-\pi/\omega_m}^{\pi/\omega_m} \frac{(\Delta f)^2 \cos\omega_m t\,dt}{(\delta f + \beta\sin\omega_m t)^2 + (\Delta f)^2}}{\int_{-\pi/\omega_m}^{\pi/\omega_m} \cos^2\omega_m t\,dt} \qquad (2\text{-}14)$$

In (2-13) and (2-14) the calculations may be simplified by finding the odd and even parts of the integrand in each numerator.

After considerable algebraic manipulation, it may be shown that d_1 is identically zero. Furthermore, when $\delta f << \Delta f$ (i.e., the oscillator frequency is very near the line center) c_1 may be shown to be given approximately by

$$c_1 \approx \frac{2\left(\frac{\delta f}{\Delta f}\right)\left(\frac{\beta}{\Delta f}\right)}{\left[1 + \left(\frac{\beta}{\Delta f}\right)^2\right]^{3/2}} \qquad (2\text{-}15)$$

Thus, a null in the output component varying at the modulation

frequency $\frac{\omega_m}{2\pi}$ is evident from (2-15) when $\delta f = 0$. Moreover, the sign associated with c_1 is dependent upon the sign of δf. A digital computer was used to evaluate (2-13) for larger values of δf. The resulting data are presented in Figure 4.

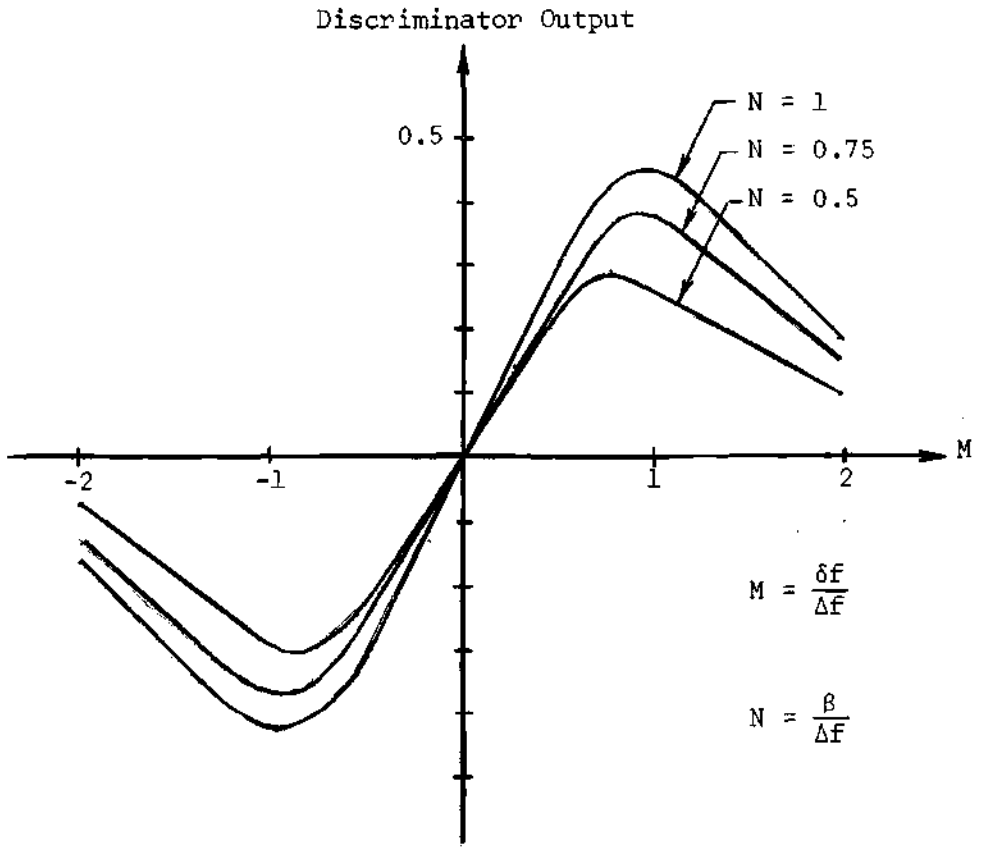

Figure 4. Calculated Discriminator Response

In the preceding discussion a single absorption line was assumed. However, as shown earlier in this chapter, lines which coincide in the absence of an applied Stark field to yield a single line, are split

apart when such a field is present. For example, the $J \rightarrow J + 1$ transition of a symmetric top molecule must consist of $(2J + 1)^2$ lines corresponding to the allowed values of K and M. However, as shown by (2-3), the observed field free resonances are independent of M. Also, positive and negative K values are not discernable. Thus, only $(J + 1)$ lines, corresponding to the number of allowed K^2 values are observed in the absence of a Stark field. The presence of M in (2-8) and (2-9), however, indicates a possible increase in the number of observed lines when a Stark field is present.

For each absorption line that shifts under the influence of a varying Stark field a discriminator characteristic may be observed. Thus, the actual discriminator curve which may be employed in a frequency control system consists of a superposition of the individual curves.

Consider, for example, a situation involving the $J = 1 \rightarrow 2$ transition of a symmetric-top molecule. Here, two moveable lines, corresponding to $MK = +1$ and $MK = -1$, are observed. One of these may be designated as the desired line, while the second is undesired. The amplitude variations due to the motion of the desired line may be assumed to be proportional to c_1 of (2-15) with δf replaced by δf_1:

$$\frac{2\left[\frac{\delta f_1}{\Delta f}\right]\left[\frac{\beta}{\Delta f}\right]}{\left[1 + \left(\frac{\beta}{\Delta f}\right)^2\right]^{3/2}}$$

From (2-8) it is evident that the two lines shift in opposite directions when a Stark field is applied. Moreover, when the applied

field is zero, the lines are coincident. Thus, the variation in α due to the desired line is cancelled by a similar, but oppositely directed, change due to the undesired line. Hence, no variation in α at the Stark frequency is observed.

If, however, it is assumed that the two lines may be separated an amount δf_2, operation near the peak of one line will be only slightly influenced by the presence of the second line when $\delta f_2 >> \Delta f$. For this case, the amplitude variations due to the undesired line may be shown to be proportional to

$$c_1' = \frac{-2\left(\frac{\beta}{\Delta f}\right)}{\left(\frac{\delta f_2}{\Delta f}\right)^3}$$

Superposition of the variations due to the two lines leads to the conclusion that the observed discriminator null occurs when

$$\frac{\delta f_1}{\left[1 + \left(\frac{\beta}{\Delta f}\right)^2\right]^{3/2}} \quad \frac{\Delta f}{\left(\frac{\delta f_2}{\Delta f}\right)^3} = 0 \qquad (2\text{-}16)$$

If, however, only the desired line were present, the null would occur when $\delta f_1 = 0$. For the null to occur close to the position of the null for a single line, the term c_1' must be small compared to c_1.

Fortunately, a dc Stark field may be applied to separate the individual ines. One of the shifted lines may then be selected as the

reference frequency. This reference frequency, therefore, differs from the molecular resonance frequency by an amount a_1E_1 Hertz, according to (2-10). Hence, the observed discriminator null occurs when

$$\frac{\delta f + a_1E_1}{\left[1 + \left(\frac{\beta}{\Delta f}\right)^2\right]^{3/2}} + \frac{1}{\left(\frac{\delta f_2}{\Delta f}\right)^3} = 0$$

In the case under consideration, the dc Stark voltage causes each line to shift a_1E_1 Hertz, but in opposite directions. Hence, the separation, δf_2, between the peaks of the two lines is merely $2a_1E_1$, and a sufficiently large value of E_1 will render the term $\left(\frac{\delta f_2}{\Delta f}\right)^{-3}$ negligible. Thus, the null, and consequently the stabilization frequency, will occur when $\delta f + a_1E_1 = 0$.

A similar procedure may be followed in cases involving more than two lines. However, both the intensity and maximum Stark induced deviation, β, of each line may be different, thus requiring appropriate changes in the expressions for the null frequency. Linear molecules may also be utilized if (2-10) is replaced by an expression of the form

$$f_o = f + \delta f + a_2(E_1 + E_2\sin\omega_m t)^2$$

where a_2 is now given by (2-76).

The above discussion outlines the method for determining the null frequency of the molecular resonance discriminator. To complete the

characterization of the device, one needs to know its slope, or frequency rate of change of the modulation frequency component of its output. For this purpose the device is assumed to be a sealed section of gas-filled waveguide, terminated with a detector to monitor the amplitude of an electromagnetic wave transmitted through the waveguide. Hence, the relationship between the modulation frequency component of the detected signal and the separation of the wave frequency from the null frequency is desired.

If one assumes that the detected voltage, e_o, is linearly proportional to the incident power, the following expression applies

$$e_o = \gamma P_i e^{-(\alpha_c+\alpha)L} \text{ volts} \qquad (2\text{-}17)$$

where

γ = detector sensitivity, volts per watt

P_i = input power to the waveguide, watts

α_c = attenuation coefficient due to waveguide losses, cm^{-1}

α = attenuation coefficient due to molecular gas, cm^{-1}

L = length of the waveguide, cm

Furthermore, since one is concerned only with the variations in e_o due to α, the component of e_o due to gaseous absorption is given by

$$\Delta e_o = \gamma P_i e^{-\alpha_c L} - \gamma P_i e^{-(\alpha_c+\alpha)L}$$

$$= \gamma P_i e^{-\alpha_c L}(1 - e^{-\alpha L})$$

Also, αL is usually small compared to unity, thereby allowing the bracketed term to be replaced by αL,

$$\Delta e_o \approx \gamma P_i e^{-\alpha_c L} \alpha L \tag{2-18}$$

From (2-15), however, the component of α that varies at the Stark modulation frequency $\frac{\omega_m}{2\pi}$ is

$$\alpha_o \left(\frac{\delta f}{\Delta f}\right)\left(\frac{\beta}{\Delta f}\right)\left[1 + \left(\frac{\beta}{\Delta f}\right)\right]^{-3/2} .$$

Replacing α in (2-18) with the term results in an expression for the amplitude of the modulation frequency component of the detected output. Hence, the discriminator slope, designated K_D, is given by

$$K_D = \frac{1}{\delta f}\Delta e_o$$

$$= \frac{2\gamma P_i e^{-\alpha_c L}\alpha_o L\left(\frac{\beta}{\Delta f}\right)}{\sqrt{2}\,\Delta f\left[1 + \left(\frac{\beta}{\Delta f}\right)^2\right]^{3/2}}, \quad \frac{\text{volts}}{\text{Hertz}} \tag{2-19}$$

where the factor $\sqrt{2}$ is required to convert from peak values to rms values. Since the modulation frequency output voltage is zero at the null frequency, Equation (2-18) relates the amplitude of a measurable voltage to the frequency separation of the molecular resonance and the frequency of the incident wave. A method for utilizing these characteristics in a practical system is discussed in the next chapter.

CHAPTER III

A MATHEMATICAL AUTOMATIC FREQUENCY CONTROL MODEL

This chapter presents a mathematical description of a typical automatic frequency control system. Although the model chosen is not unique, it provides insight into the use of a molecular discriminator in a feedback control loop.

As shown in the preceding chapter, the error signal appears as a modulation on an ac carrier voltage. Hence, the system may be classified as a carrier-type servo-system. For analytical purposes, however, the error signal is assumed to be the demodulated information contained on the carrier, the details of the demodulation process being presented in a later chapter. The effect of various parameters on both short- and long-term stability* is investigated. Furthermore, the relationship of the amplifier gain and bandwidth to the closed loop transfer function is discussed.

The molecular resonance stabilization method may be represented, as shown in Figure 5, by a block diagram having two inputs and a single output. The inputs are the molecular resonance frequency and the frequency of the oscillator when the feedback loop is opened. The output

---

*Since the time intervals involved in short- and long-term stability measurements have never been clearly specified, it will be arbitrarily assumed that *short-term* applies to averaging intervals of one second or less and that *long-term* applies to averaging times much greater than one second.

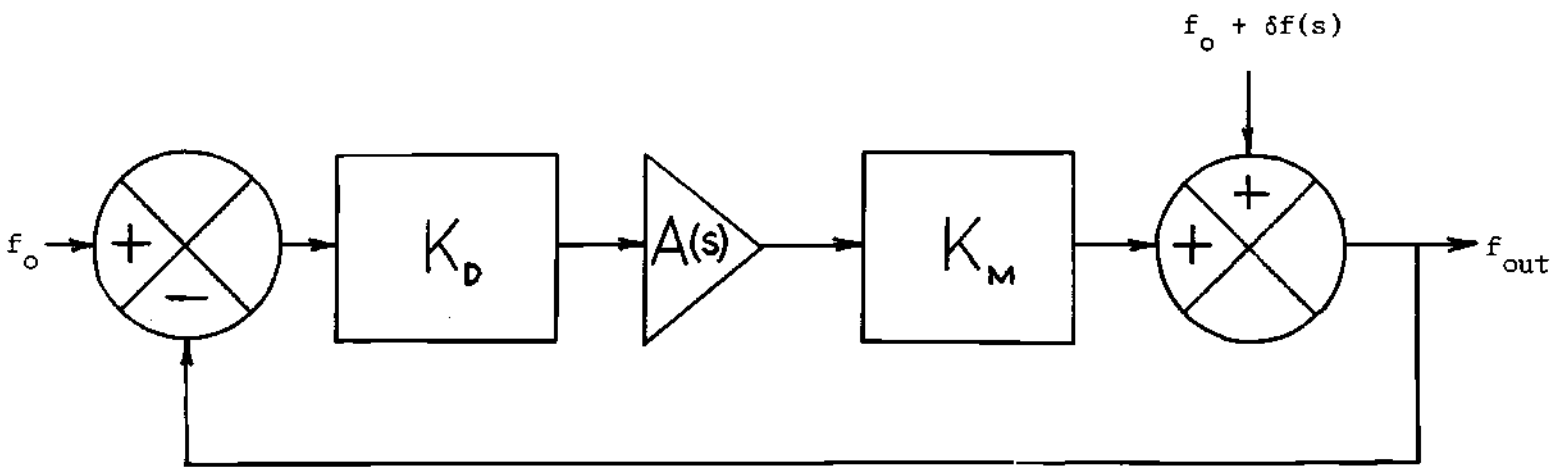

Figure 5. An AFC Mathematical Model

is the closed loop frequency of the oscillator. Thus the transfer function of this system may be represented in Laplace transform notation by

$$\frac{f_{out}(s) - f_o(s)}{\delta f_o(s)} = \frac{1}{1 + A(s)K_D K_m} \tag{3-1}$$

where

f_{out} = stabilized klystron frequency

f_o = molecular transition frequency

δf = open-loop error between the klystron and reference frequencies

A = amplifier gain

K_D = molecular discriminator slope

K_m = klystron modulation sensitivity.

Of particular interest is the steady state error $\lim_{t\to\infty}(f_{out}(t) - f_o)$ which occurs for various open loop errors $\delta f_o(t)$. This error may be readily obtained through application of the Final Value Theorem (13). Thus, for the case where $\delta f_o(t)$ suddenly increases from zero to a constant value, d, at $t = 0$ the steady state error may be shown to be

$$\lim_{t\to\infty} (f_{out}(t) - f_o) = \lim_{s\to 0} \frac{s\,\frac{d}{s}}{1 + A(s)K_D K_m} = \frac{d}{1 + A(0)K_D K_m} \tag{3-2}$$

It is evident from (3-2) that the error may be arbitrarily small provided that the dc loop gain $1 + A(0)K_D K_m$ can be made sufficiently large.

If, however, noise is assumed to be present at the discriminator output, the block diagram must be modified as shown in Figure 6. Assuming the noise voltage to be V_n, the applicable transfer function is

$$f_{out}(s) - f_o(s) = \frac{\delta f_o(s)}{1 + A(s)K_D K_m} + \frac{AK_m V_n(s)}{1 + A(s)K_D K_m} \qquad (3\text{-}3)$$

For a loop gain much greater than unity, the term containing V_n may be replaced by V_n/K_D. Therefore, the minimum frequency error is determined by the noise voltage and the discriminator slope as well as the open loop error δf. It should be noted, however, that the noise voltage V_n will usually have a zero mean value so that the long-term average frequency will be determined primarily by the open-loop error. The short-term stability, though, will depend on the instantaneous fluctuations in V_n. Hence it is desirable to minimize the term V_n/K_D.

The presence of noise at the terminals of the absorption cell output detector requires that one consider a region of uncertainty in the vicinity of the discriminator null, as shown in Figure 7. Thus, for signal voltages whose magnitudes are less than the noise voltage V_n, the frequency error producing this signal is indeterminate. The minimum detectable frequency error is therefore V_n/K_D. Hence, the quantity $\pm V_n/K_D f_o$ represents the maximum short-term stability (minimum fractional frequency error) that may be achieved by the system when δf has no rapid time variations.

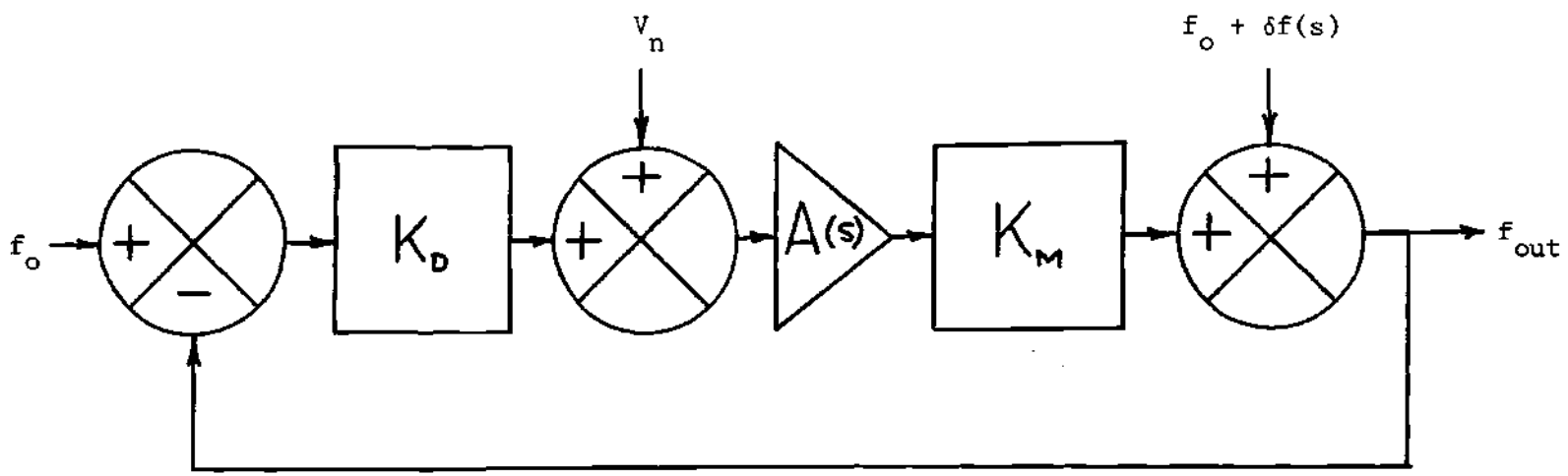

Figure 6. An AFC Mathematical Model Including Noise Input

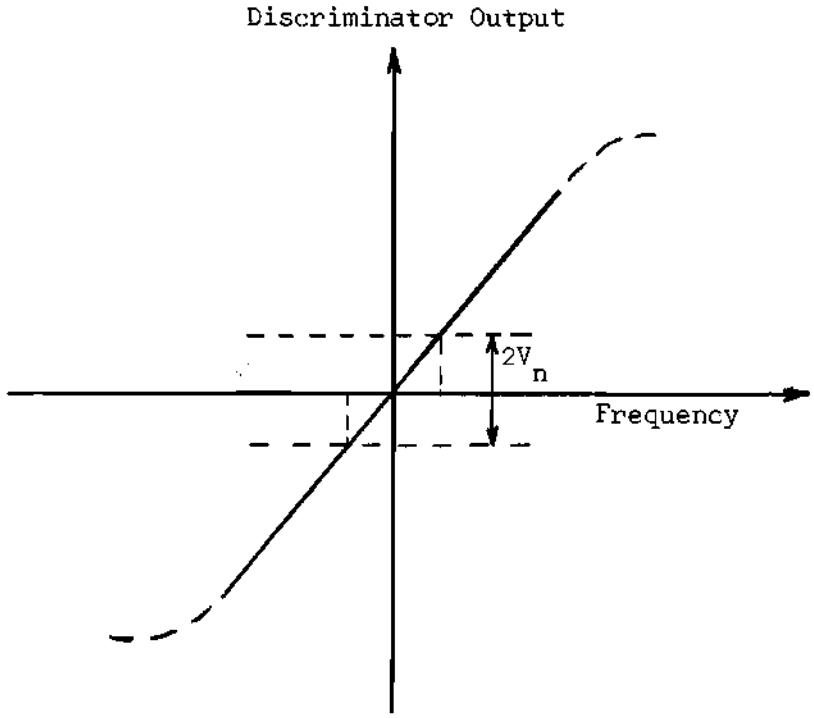

Figure 7. Discriminator Null Ambiguity Due to Noise

Moreover, since α_o and Δf are functions of the electromagnetic power P_i (14), an optimum line width Δf_{opt} may be selected for a given power to maximize K_D. The relationships between α_o, Δf, and P_i demonstrating the saturation of the absorption coefficient and observed linewidth are given by

$$\alpha_o' = \alpha_o \frac{1}{1 + CP_i}, \qquad cm^{-1} \tag{3-3}$$

and

$$\Delta f' = \Delta f\sqrt{1 + CP_i} \quad , \qquad \text{Hz} \tag{3-4}$$

The primed values represent saturated parameters and the constant C is equal to

$$\frac{8\pi|\mu_{01}|^2}{3ch^2S(\Delta f)^2} \times 10^7 \quad ,$$

where $|\mu_{01}|^2$ is the square of the effective dipole moment matrix element for the desired transition and S is the cross-sectional area of the waveguide absorption cell in square centimeters.

Inserting (3-3) and (3-4) into Equation (2-18) and setting $\partial K_D/\partial(\Delta f) = 0$, the value of Δf which maximizes K_D may be obtained. This value, Δf_{opt}, is found to be

$$\Delta f_{opt} = \sqrt{\frac{16\pi|\mu_{01}|^2 P_i \times 10^7}{3ch^2S}} \tag{3-5}$$

and the resulting value of K_D is

$$K_{D,max} = \frac{\gamma P_i \alpha_o L\, e^{-\alpha_c L}}{(1.5)^3\sqrt{\frac{16\pi|\mu_{01}|^2 P_i \times 10^7}{3ch^2S}}} \quad , \quad \frac{\text{volts}}{\text{Hertz}} \tag{3-6}$$

An additional increase in $K_{D,max}$ may be obtained by operating at lower temperatures. For a symmetric-top molecule, it has been shown that the absorption coefficient varies as $T^{-5/2}$. Thus, assuming that

the pressure is adjusted for the optimum linewidth as temperature is decreased, the discriminator slope, and hence stability, may be substantially increased.

The noise voltage, V_n, may be due to a combination of random fluctuations in the klystron output, noise in the detector itself, or noise generated within the amplifier connected to the detector. Häggblom (15), however, has shown that amplitude modulation noise in reflex klystrons is generally much greater than 120dB below the carrier power for a one Hz bandwidth separated from the carrier frequency by more than one kHz. Thus, even for bandwidths of several hundred Hz, the oscillator noise power will be greater than 100dB below the desired carrier power and may be neglected. Then, assuming that the detector may be represented as a voltage source in series with a video resistance R_v, the noise voltage may be predicted by an expression of the form

$$V_n = \sqrt{4ktTR_vB} \quad , \quad \text{volts} \qquad (3\text{-}7)$$

where

k = Boltzmann's constant

t = effective noise temperature ratio (including the effects of rectified or applied bias and amplifier noise)

T = ambient temperature

B = effective noise bandwidth to the system.

Recalling from (3-3) that the rapid variations in the closed-loop frequency are given approximately V_n/K_D, the fractional short-term

stability is

$$\frac{V_n}{K_D f_o} = \frac{\sqrt{4ktTR_v B}}{K_D f_o} \quad . \tag{3-8}$$

To further characterize the system one needs to determine the response of the system to various functions, $\delta f_o(t)$. For this purpose, the spectral shape of the amplifier response must be included in the system equations. In one of its most simple forms, the loop amplifier may be represented by a simple low-pass function:

$$A(s) = \frac{A_o w_1}{s + w_1}$$

Hence, the system transfer function, or ratio of the closed loop frequency deviations to the open loop deviations is given by

$$\frac{f_{out}(s) - f_o}{\delta f_o(s)} = \frac{s + w_1}{s + (1 + A_o K_D K_m) w_1} \tag{3-9}$$

A plot of this function is shown in Figure 8. From this figure it is evident that the output deviation will always be smaller than any periodic open-loop deviation δf_o. As the frequency of a periodic variation approaches zero, the magnitude of the output deviation approaches a value equal to the open-loop deviation divided by the dc loop gain.

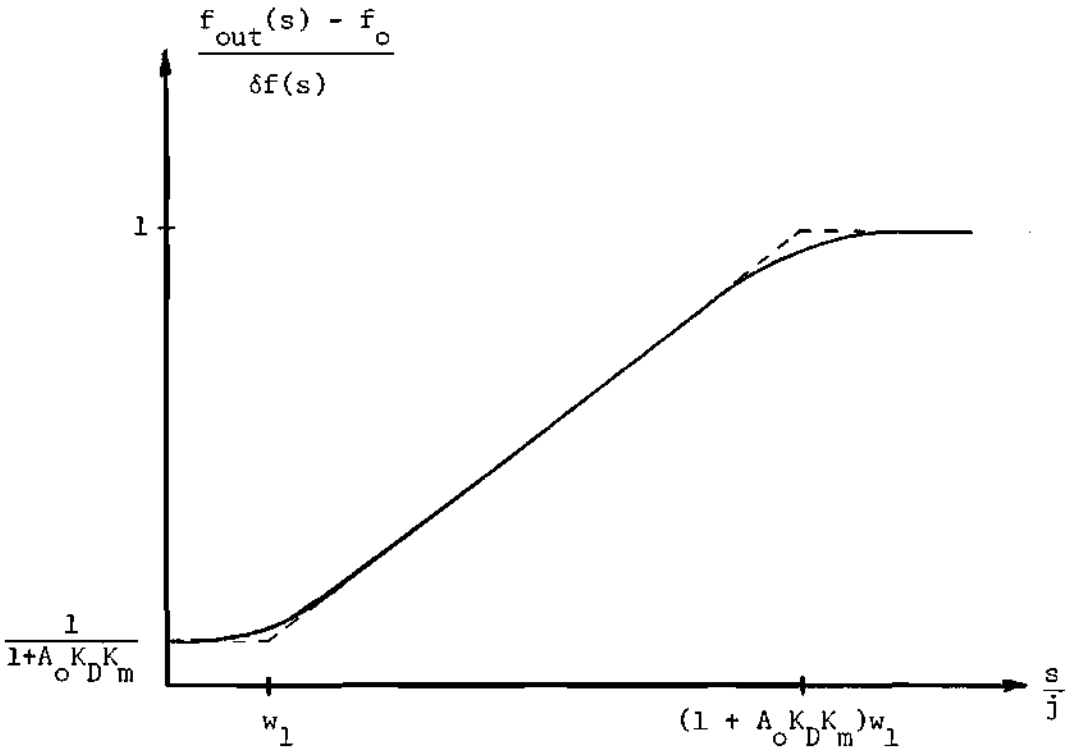

Figure 8. The Loop Transfer Function for a Single Pole Amplifier System

On the other hand, as the frequency of the variation is δf_o is increased, the loop gain is reduced, thereby allowing closed-loop deviations to approach the open-loop level.

In many cases the gain function actually employed is slightly more complicated than the simple low-pass function described above. For instance, a second break-frequency, w_2, above which an increased roll-off in gain occurs, may be employed to further reduce such undesirable

signals as harmonics of the modulation signal. Hence, an amplifier gain function of the form,

$$A(s) = \frac{A_o w_1 w_2}{(s + w_1)(s + w_2)} \tag{3-10}$$

may be assumed. The resulting ratio of the closed and open loop deviations is therefore,

$$\frac{f_{out}(s) - f_o}{\delta f_o(s)} = \frac{(s + w_1)(s + w_2)}{s^2 + s(w_1 + w_2) + (1 + A_o K_D K_m) w_1 w_2} \tag{3-11}$$

For analytical purposes, the right-hand side of (3-11) may be recast in the form of a partial fraction expansion:

$$\frac{f_{out}(s) - f_o}{\delta f_o(s)} = 1 + \frac{K_1}{s + s_1} + \frac{K_2}{s + s_2} \tag{3-12}$$

where K_1 and K_2 are constants, and s_1 and s_2 are the roots of the denominator of (3-11). For any given $\delta f_o(t)$, the output error $f_{out}(t) - f_o$ may be computed from (3-12).

The roots s_1 and s_2 are given by

$$s_1, s_2 = \frac{(w_1 + w_2) \pm \sqrt{(w_1 + w_2)^2 - 4(1 + A_o K_D K_m) w_1 w_2}}{2}$$

Since $A_o K_D K_m$, w_1, and w_2 are positive numbers,

$$(w_1 + w_2)^2 - 4(1 + A_o K_D K_m) w_1 w_2 < (w_1 + w_2)^2 \ .$$

Hence, the roots s_1 and s_2 will have negative real parts for all values of w_1 and w_2 and the system response to a step discontinuity in $\delta f_o(t)$ remains bounded.

If w_2 is assumed equal to w_1, it is evident that for real frequencies ($s = jw$) the phase of $A(jw)$ in (3-10) rapidly approaches 180° for frequencies only a few times w_1. Therefore, slight deviations in the system may allow the phase to reach 180° and produce an unstable response.

However, if one assumes that the amplifier response is essentially a single pole function with increased roll off in gain at frequencies considerably above the -3dB low-pass frequency (i.e., $w_2 >> w_1$) the roots s_1 and s_2 are given approximately by

$$s_1, s_2 \approx -\frac{w_2}{2} \pm \frac{w_2}{2} \sqrt{1 - 4(1 + A_o K_D K_m) \frac{w_1}{w_2}}$$

A plot of the loci of these roots as a function of the dc loop gain $(1 + A_o K_D K_m)$ is shown in Figure 9. For $1 - 4(1 + A_o K_D K_m) w_1/w_2 < 0$, the roots are obviously complex and have a fixed negative real part. As the loop gain is decreased, a point is reached where

$$1 - 4(1 + A_o K_D K_m) \frac{w_1}{w_2} = 0$$

and the roots then become equal, real, and negative.

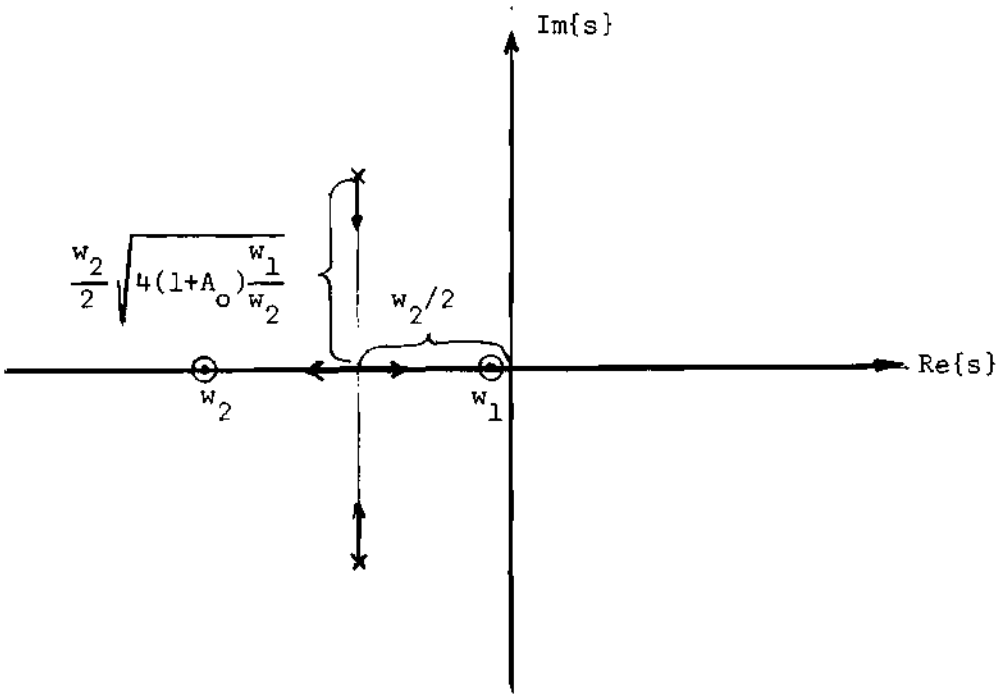

Figure 9. Root Locus Plot of a Two-Pole Amplifier System

For any lower loop gain, the roots remain real and negative, but separate from each other along the negative real axis. To ensure that the ratio of closed-loop deviations to open-loop deviations is minimized for all real frequencies, the roots s_1 and s_2 should both be as large as possible. An obvious method for achieving this is to make w_2 large.

To provide sufficient loop gain for the suppression of rapid open loop variations w_1 must be large. Noise within the system, however, may require that narrow bandwidths (small w_1) be employed. As evidenced by Figure 9, this provides improved long-term stability, but may have negligible effect on the short-term stability. With sufficiently noise

free detectors and amplifiers, w_1 may be made large enough so that oscillator frequency deviations due to power supply ripple or other rapid perturbations can be cancelled.

To evaluate the performance of a specific system, it is evident from the above discussion that a number of system parameters must be known. In the next chapter, the methods by which numerical values may be assigned to these parameters will be discussed.

CHAPTER IV

EXPERIMENTAL PROCEDURES AND PRELIMINARY DATA

The techniques of frequency measurement depend, to a large extent, on the portion of the spectrum in which the measurements are to be made. At low frequencies, the period of oscillation may be directly observed. In the radio frequency region, passive discriminators and period measurements may be employed. At microwave frequencies heterodyne measurements utilizing an oscillator of known characteristics is often used to produce a low frequency beat note. Then, direct measurement of the period of the low frequency note yields information which may be used to characterize the microwave oscillator. In each case, however, either a known time or frequency standard must be employed.

A complete specification of an oscillator's characteristics will usually include three items: (1) absolute frequency, (2) short-term stability, and (3) long-term stability. With appropriate modifications, the methods mentioned above may be used for measurement of these characteristics. Extreme precision, however, can be guaranteed only if the reference possesses satisfactory characteristics. Thus, the reference should have characteristics which are at least an order of magnitude better than the expected values of the corresponding characteristics of the oscillator under examination.

A knowledge of the absolute frequency is often of far less

significance than the variations of the oscillator frequency about an established operating frequency. Thus, a reference having a known stability, but whose absolute frequency is not precisely known, may be employed to characterize the stability of the given oscillator. In the example under consideration, several measurements will be made which utilize a rotational resonance of methyl fluoride, CH_3F, as a reference. This reference frequency will be assumed to be stable, based on natural laws governing molecular motion. Additional frequency measurements will employ a low frequency temperature-stabilized crystal oscillator as the basis for comparison.

Determination of the ultimate stability which might be achieved through employment of the molecular frequency discriminator in an oscillator control system requires a knowledge of several parameters. Of primary concern are the parameters which describe the molecular behavior, the characteristics of the silicon-crystal detector, and the inherent instability of the oscillator. In the following paragraphs, these characteristics, techniques for measuring them and certain previously unused frequency measurement techniques will be discussed.

Detector Characteristics

The silicon crystal detector, employed in several of the preliminary measurements, as well as in the stabilization system, will be examined first.

According to Uhlir (16) and Whitford (17), the silicon crystal detector employed at the output of the absorption cell may be characterized by an equivalent circuit consisting of a voltage source in series

with a resistance. The open circuit voltage is directly proportional to the power incident on the detector, the proportionality constant being designated γ. Moreover, the resistance is nearly constant over a wide range of incident power levels and, for computational purposes, a real resistance of R_v ohms may be assumed.

Measurement of γ requires a knowledge of the power incident on the detector. For this purpose, a calibrated bolometer and modulated source, shown in Figure 10 was employed. The output of the klystron is turned on and off, at a 1000 Hz rate by applying a square wave modulation voltage to the reflector. Adjustment of the power level incident on either the bolometer (TRG-W990) or the silicon crystal detector is accomplished by setting the calibrated adjustable attenuator. To determine the output of the attenuator, a bias current of four milliamperes dc was applied to the bolometer and the voltage developed across the unit was observed with the oscilloscope. According to the manufacturer's specifications, the bolometer resistance changes about 7.5 ohms for each milliwatt of applied power. Thus, application of a one milliwatt rf signal should provide a change in voltage across the bolometer of about 30 millivolts. Since the signal is turned completely off and back on again 1000 times per second, the voltage present at the oscilloscope should be square-wave modulated, the amplitude of the modulation being directly proportional to the change in incident power as the source is switched off and on.

Based on the above power level calibration, the silicon crystal detector may be substituted for the bolometer and the detector sensitivity γ determined. A plot of the crystal output as measured by a high

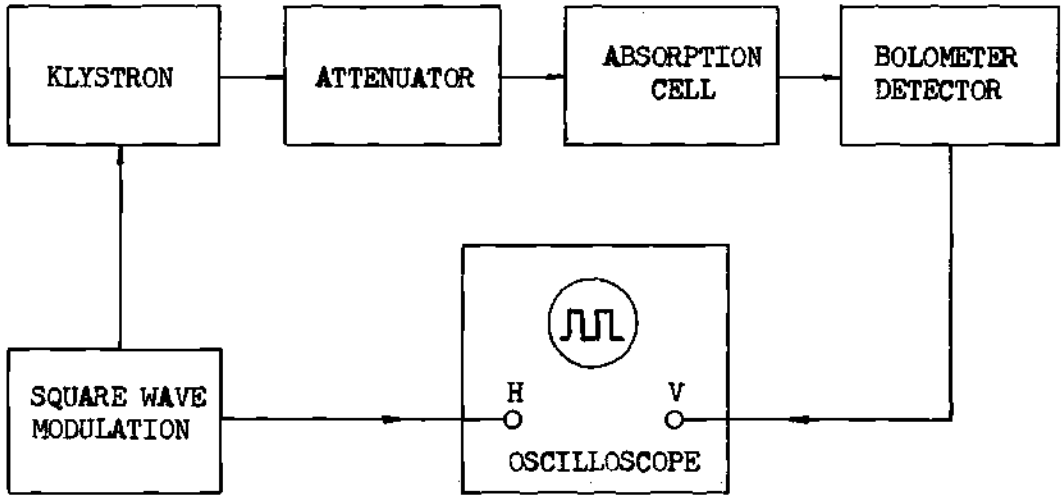

Figure 10. Power Level Calibration Set-up

input impedance oscilloscope versus incident power is shown in Figure 11. The slope of the curve represents the detector sensitivity γ and is approximately 100 volts/watt. It should be noted, however, that a dc bias of about 25 microamperes was required to maintain this sensitivity at modulation frequencies greater than a few kiloHertz.

The value of the resistance R_v is determined by loading the output of the crystal detector with a resistance R while observing the peak to peak variations of the modulated signal with the oscilloscope. As R is decreased from infinity to a certain value, the peak to peak voltage at the input of the oscilloscope will decrease to one half the open circuit value. For this particular condition $R = R_v$. The value obtained in this manner, experimentally, is about 5000 ohms and is independent of power for levels below about one milliwatt. Several 1N53 crystals were examined and each exhibited R_v values near 5000 ohms while the values of γ varied by as much as a factor of five.

Molecular Characteristics

The resonant frequencies of various molecular transitions in the region of two to three millimeters wavelength have been investigated by Johnson et al. (18). Their results show that the transition frequencies of methyl fluoride are 102, 142.62 ± .20 and 102, 140.85 ± .20 MHz for the $J = 1 \rightarrow 2$, $K = 0$ and $J = 1 \rightarrow 2$, $|K| = 1$ transitions, respectively.

Additional molecular parameters, such as the permanent dipole moment μ, the line width parameter Δf, measured at one mmHg pressure, and the symmetry axis rotational constant C, are tabulated in Appendix VI of (8) for numerous molecules. For methyl fluoride, μ, Δf, and C are

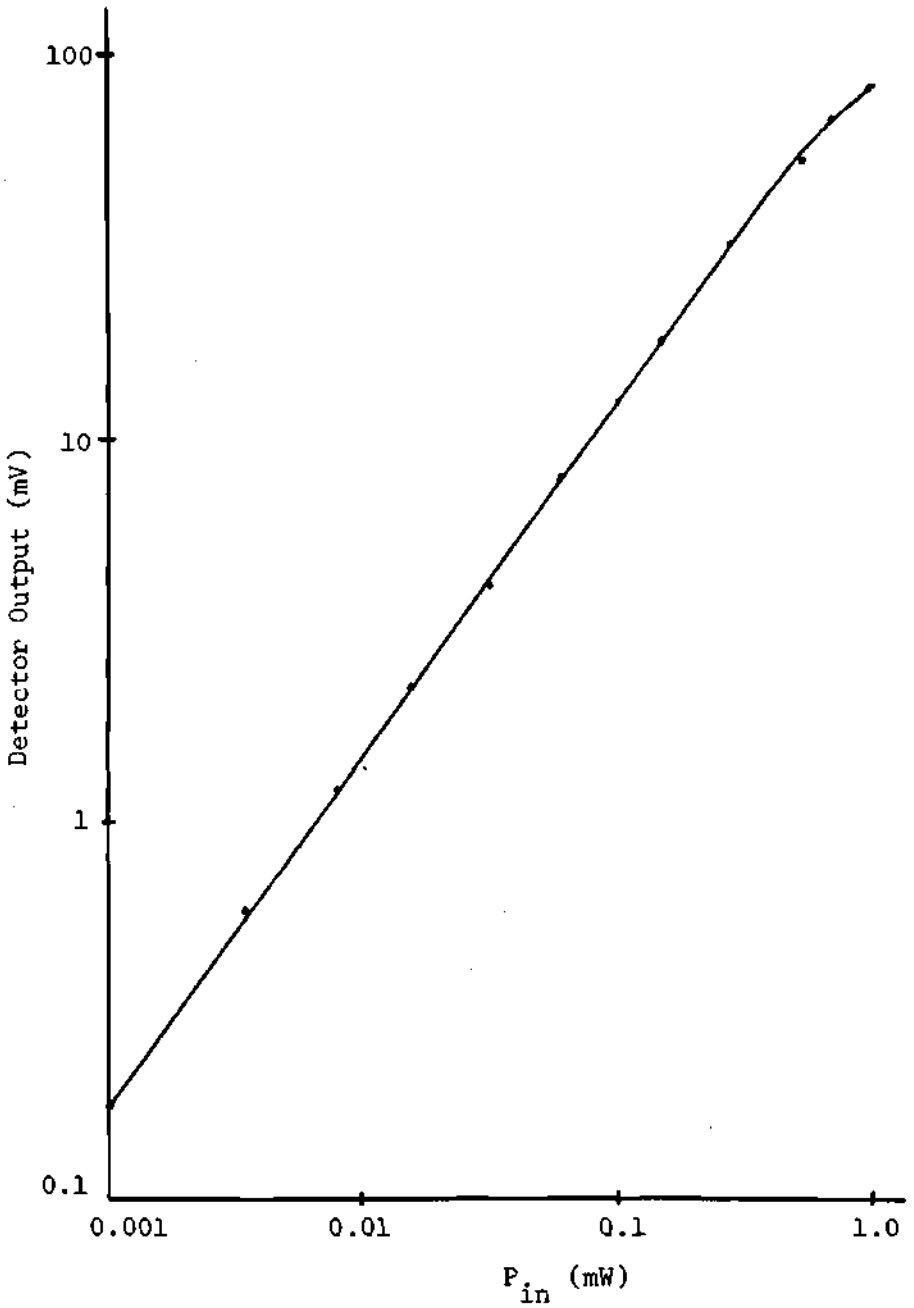

Figure 11. Observed Detector Voltage versus Input Power

1.79 Debye*, 20 MHz, and 154,000 MHz, respectively.

Line Intensities

Observed values of the line intensities are not available in the literature. However, values were calculated and then compared with those obtained in the laboratory.

The following expression was used to predict the maximum value of the absorption coefficient α:

$$\alpha_{max} = \frac{1.23 \times 10^{-20} f_v S(I,K) \sqrt{C}\, \mu^2}{4I^2 + 4I + 1} \left[1 - \frac{K^2}{(J+1)^2}\right] \frac{f_o^3}{\Delta f} \text{ cm}^{-1} \qquad (4\text{-}1)$$

where

f_v = fraction of molecules in vibrational state of interest,

$\frac{S(I,K)}{4I^2 + 4I + 1}$ = statistical weighting factor,

I = spin quantum number of off axis atoms,

C = rotational constant about symmetry axis, MHz,

μ = dipole moment, debye units,

Δf = half line width at half maximum at one mmHg pressure, MHz,

f_o = resonant frequency, MHz,

and the temperature is assumed to be 300°K.

---

*1 Debye = 10^{-18} electrostatic units.

The statistical weighting factor $S(I,K)/4I^2 + 4I + 1$ is required in (4-1) to account for degeneracy of the energy levels due to atomic spin and inversion. A detailed discussion of Equation (4-1) and the statistical weighting factor is presented by Townes and Schawlow (19). For methyl fluoride, having three identical atoms off the symmetry axis, the statistical weighting factor is 3/2 for both the $K = 0$ and $|K| = 1$ lines.

In addition, a knowledge of the individual vibrational modes of the molecule is required for the computation of the parameter f_v. The frequencies of the vibrations of methyl fluoride are also tabulated by Townes and Schawlow (20). Referring again to (19), it may be shown that f_v is nearly unity at room temperatures.

Thus, the maximum absorption coefficient of methyl fluoride, CH_3F, is given by

$$\alpha_{max} = 1.2 \times 10^{-3} \left[1 - \frac{K^2}{(J+1)^2}\right] \text{ cm}^{-1} \qquad (4\text{-}2)$$

To be consistent with the notation of microwave spectroscopy, J in (4-1) and (4-2) represents the smaller of the two values involved in a particular transition. Hence, the intensity of the $K = 0$ line is characterized by a peak absorption coefficient of about 1.2×10^{-3} cm^{-1} while the peak intensity of the $|K| = 1$ line is about 0.9×10^{-3} cm^{-1}.

Verification of the intensities thus predicted was achieved by monitoring the detected voltage at the output of an absorption cell as the signal source was slowly swept in frequency through the molecular

resonance. A pressure of 0.5 mmHg was sustained within the waveguide cell throughout the measurement. Since the line width at this pressure is 10 MHz, the lines for K = 0 and $|K| = 1$ cannot be distinguished. Therefore, the observed intensity should be approximately equal to the sum of the intensities of the individual lines.

Recalling expression (2-16), which has been experimentally verified, the voltage out of the detector is given by

$$e_o = \gamma P_i e^{-(\alpha_c+\alpha)L}$$

Then, if α_c and P_i are independent of frequency over a range of frequencies near the molecular resonance frequency f_o, the peak line intensity may be determined by measuring e_o at a frequency where α is negligible and again at the frequency f_o. Since $\alpha = \alpha_o$ at $f = f_o$, the difference δe_o in the voltages thus measured is given by

$$\delta e_o = \gamma P_i e^{-\alpha_c L} - \gamma P_i e^{-(\alpha_c+\alpha_c)L} \qquad (4\text{-}3)$$

$$= \gamma P_i e^{-\alpha_c L}(1 - e^{-\alpha_o L})$$

For $\alpha_o L \ll 1$, typical of most observed molecular absorption, (4-3) may be approximated by

$$\delta e_o \approx P_i e^{-\alpha_c L} \alpha_o L \qquad (4\text{-}4)$$

Furthermore, $\gamma P_i e^{-\alpha_c L}$ represents the maximum detector voltage, $e_{o_{max}}$, which occurs when the absorption due to the gas is negligible. Thus, Equation (4-4) may be rewritten in the form

$$\alpha_o = \frac{1}{L} \frac{\delta e_o}{e_{o_{max}}}$$

The experimentally observed value of $\delta e_o / e_{o_{max}}$ was found to be 0.12 for CH_3F. The cell length used in 122 cm, thereby yielding a value of 10^{-3} cm^{-1} for α_o. This is approximately one half of the value predicted by the combined intensities of the K = 0 and $|K|$ = 1 lines predicted from (4-2).

Since the absorption line employed in the stabilization system is obtained by Stark splitting of the $|K|$ = 1 line, a line intensity which is less than that of the field-free $|K|$ = 1 line is expected. Recognizing that the intensity of a particular transition is proportional to the difference in populations of the upper and lower energy states involved in the transition, it may be shown that the MK = 1 line should be 9/70 of the combined intensity of the K = 0 and $|K|$ = 1 lines. Experimental observations show the peak intensity of the MK = 1 line to be approximately 1/8 of the total field-free intensity, or about 0.125×10^{-3} cm^{-1}. Hence, the relative magnitude of the Stark shifted line is in close agreement with the theoretically predicted fraction.

Stark Shift

The magnitude of the frequency shift produced by the Stark field is readily obtained by inserting the known value of the molecular dipole

moment in Equation (2-8). In addition, the dimensions of the Stark cell (Figure 12), described in detail in Chapter V, may be used to calculate the Stark Field intensity E as a function of the applied voltage V_s; hence,

$$E = 1.56\ V_s \times 10^{-2}\ \text{e.s.u.}^*$$

where V_s is measured in volts. The resulting expression for the Stark shift is

$$\delta f_{Stark} = \frac{2MK}{J(J+1)(J+2)} \frac{\mu E}{h} = 1.4\ V_s\ \text{MHz} \qquad (4\text{-}5)$$

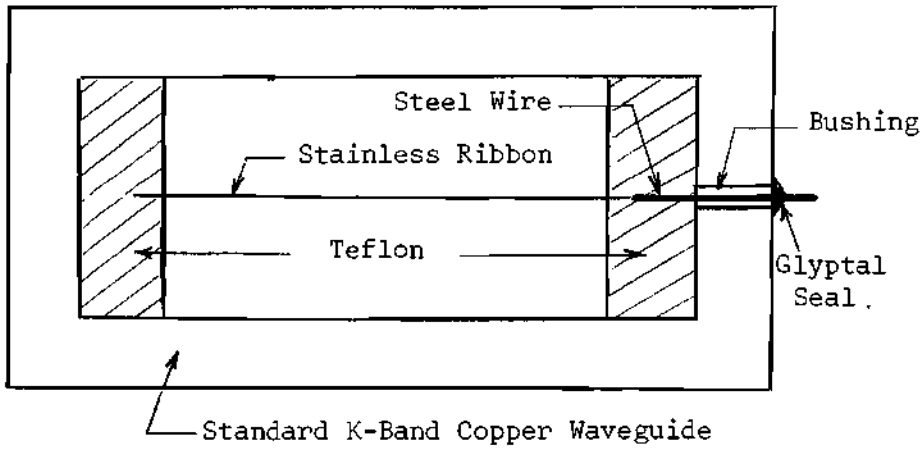

Figure 12. Stark Cell Cross-Section

*e.s.u. or electrostatic units = volts/cm divided by 300.

Experimental verification of Equation (4-5) was obtained by direct observation of the frequency shift produced by a known voltage applied to the Stark cell. Utilizing the discriminator action of either the MK = +1 or MK = -1 lines, the klystron frequency was adjusted to provide a null in the fundamental frequency component present at the absorption cell output detector for several values of applied dc Stark voltage. Each value of applied voltage was measured with a digital voltmeter and the klystron frequency shift was noted on a calibrated spectrum analyzer having a stability of at least a few kiloHertz per minute.

Further experimental verification of Equation (4-5) was achieved by utilizing the known separation (1.76 MHz) of the K = 0 and |K| = 1 lines in the absence of the Stark field. Reduction of the pressure in the absorption cell to a sufficiently low pressure allows the K = 0 and |K| = 1 lines to be resolved on a swept frequency oscilloscope presentation. The separation of the two observed peaks thus enables the horizontal scale of the oscilloscope to be calibrated in frequency, as shown in Figure 13. Application of a static Stark field will then split the |K| = 1 line into three components, one of which remains stationary and two that shift in opposite directions. The separation of the oppositely shifted lines is simply twice the shift of one line and may be readily determined from the calibrated oscilloscope scale. From this observed separation and the known value of applied voltage Equation (4-5) may be verified. The data thus obtained indicates that both methods agree with the theoretical expression to within 10 per cent.

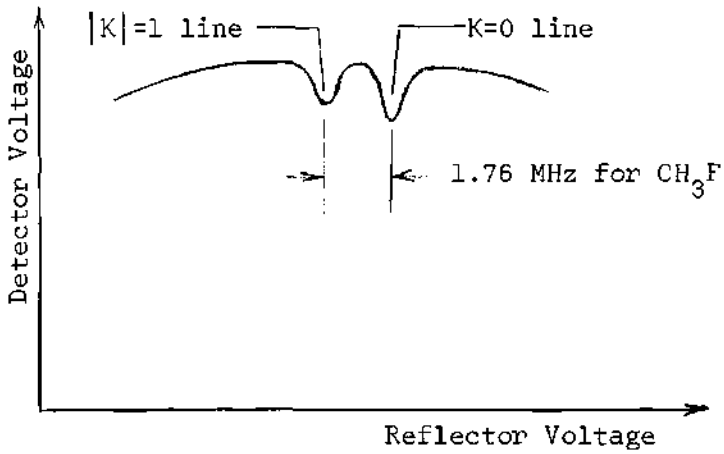

Figure 13. Typical Oscilloscope Presentation of K = 0 and |K| = 1 Lines

Inherent Klystron Stability

In the absence of adequate facilities for direct comparison of the stabilized and unstabilized oscillator frequencies with a primary frequency standard, two methods of relative frequency comparison were selected. The first method is based on the assumed stability of the microwave molecular transition frequencies while the second method employs a spectrum analyzer having an internal reference, or secondary standard with a specified stability. In each case, absolute frequency measurements are not possible, but the relative separation of oscillator frequency and the reference may be readily determined.

The discriminator characteristics of the molecular resonance lines provide the basis for the first method of frequency measurement. These

resonance lines may be used either by calibrating the slope of the discriminator response or by tuning the null frequency of the discriminator through variation of the dc component of the Stark field. In situations where the total frequency drift of the source over periods of a few hours exceeds one or two linewidths, the latter method has proven to be quite satisfactory. However, the magnitude of the dc component of the Stark field and the coefficient relating the magnitude of this component to the shift in the null frequency must be accurately known. Calibration of this dc Stark shift has already been discussed.

The use of the calibrated slope, or nontracking discriminator, is acceptable in situations where it is known *a priori* that the frequency drift of the signal source will lie between the positive and negative peaks of the discriminator curve. For frequencies outside of this range, the multivalued nature of the curve introduces an undesirable ambiguity into the measurements. This method of measurement, however, may be readily employed for determination of the drift of a stabilized oscillator when the probability that the stabilized frequency will deviate from the null by more than a linewidth is negligible.

A plot of observed frequency drift over a period of two hours is presented in Figure 14. The data were obtained by tracking the null and converting the dc Stark voltage to an equivalent frequency drift by means of Equation (4-5).

Further characterization of the unstabilized klystron was obtained by the spectrum analyzer method. This method of frequency determination is based on a measurement of the beat frequency produced by mixing a harmonic of a highly stable low frequency oscillator and the output of

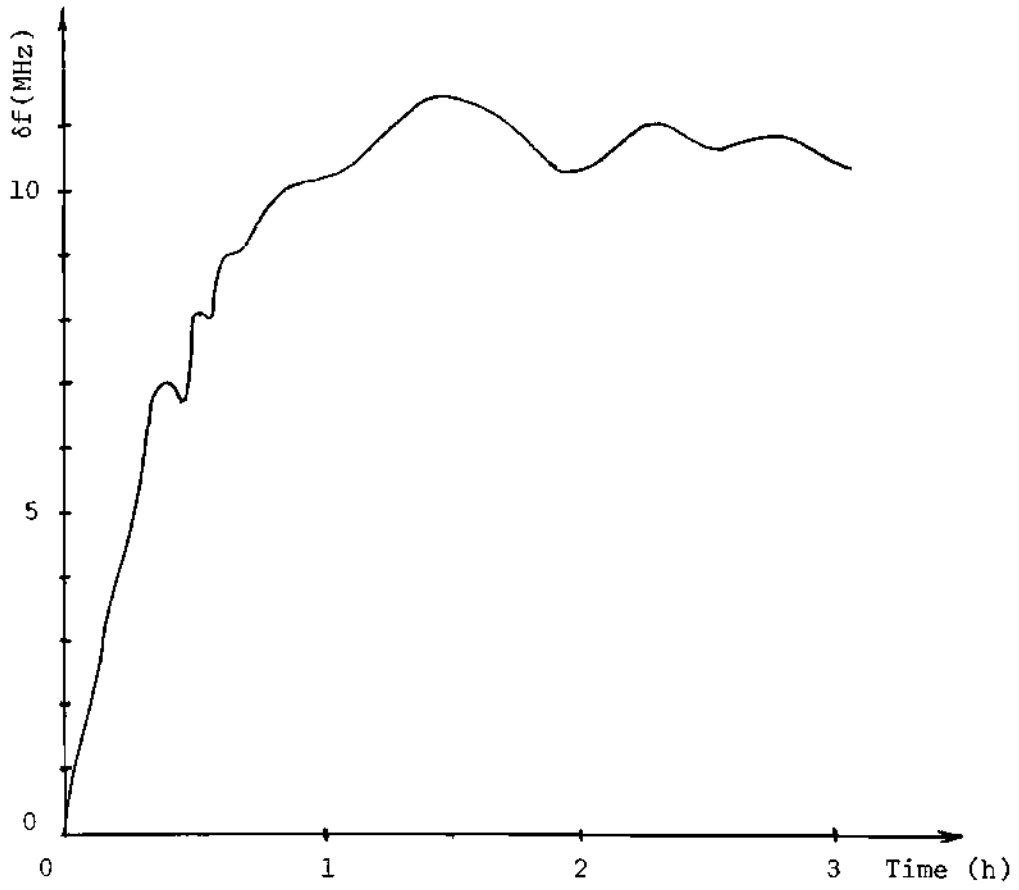

Figure 14. Observed Open-Loop Drift--Null Tracking Method

the klystron. The Polarad Model 2992A Spectrum Analyzer utilized for this measurement employs a backward wave oscillator (BWO) which is phase locked to a harmonic of a crystal oscillator. The crystal frequency is approximately 30 MHz and may be electrically tuned over a small range. This arrangement, according to the manufacturer, has a stability of a few parts in 10^9/second while the claimed stability

for periods of an hour is one part in 10^6. Thus, frequency drifts of the order of one MHz at a nominal operating frequency of 100 GHz should be readily observable. A plot of observed klystron stability utilizing the spectrum analyzer is shown in Figure 15.

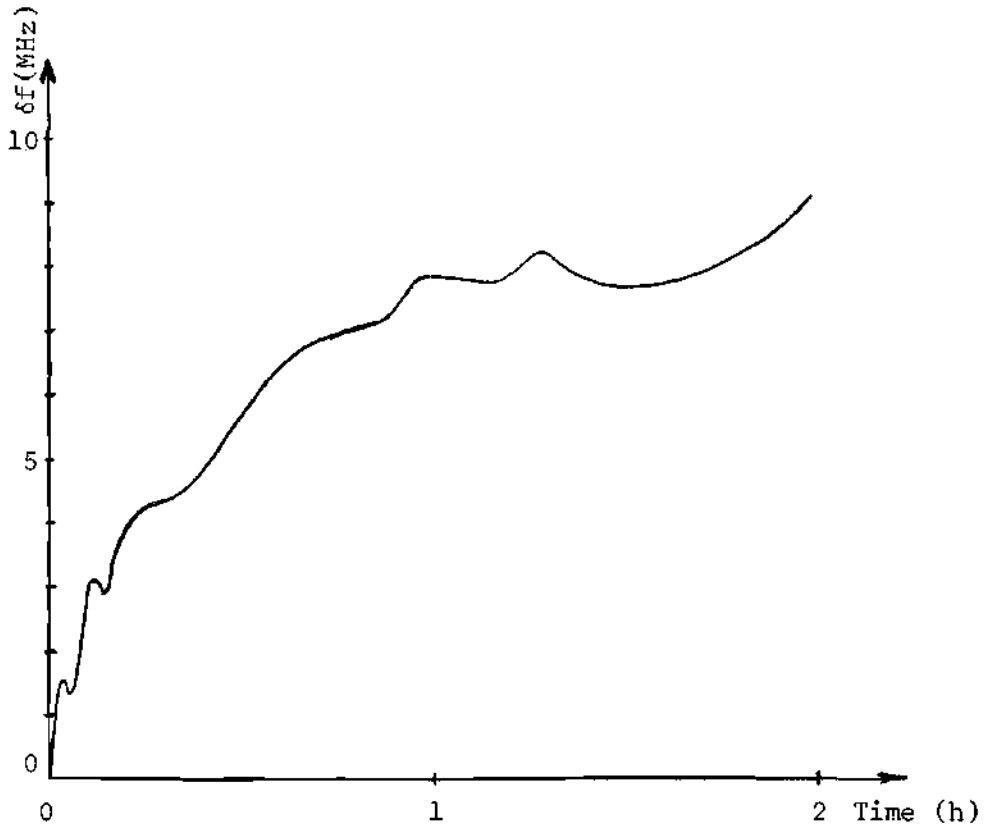

Figure 15. Observed Open-Loop Drift--
Spectrum Analyzer Method

Each of the methods used indicated that frequency drifts of one or more MHz may occur over periods of a few seconds to a few minutes,

even after an hour of warm up time. It should be noted, however, that no attempt was made to stabilize the temperature of the klystron other than that achieved by forced air cooling.

In the next chapter, an experimental AFC system, based on methyl fluoride, will be discussed. Utilizing data presented above, the mathematical model will be used to predict the performance of the system. The predicted performance will then be compared with experimental results.

CHAPTER V

AN EXPERIMENTAL METHYL FLUORIDE AFC SYSTEM

A stabilization system based on the molecular frequency discriminator was constructed at Georgia Tech under NASA Institutional Grant NsG-657. The system has been used to stabilize a reflex klystron oscillator at a frequency of approximately 102 GHz. The $J = 1 \rightarrow 2$ rotational transition of methyl fluoride, CH_3F, was used to provide the required discriminator characteristics.

The stabilization system consists of a millimeter signal source, waveguide components, a specially constructed waveguide absorption cell, and various signal processing devices. In addition, a vacuum pump and facilities for filling the waveguide cell with the gas were utilized. Figure 16 is a simplified diagram of the complete stabilization system showing interconnections of the various components.

The frequency control voltage for the signal source was developed by processing a sample of the oscillator output. Various waveguide components were used to obtain the sample and control its level. The sample was then passed through the gas-filled waveguide absorption cell. Application of an alternating electric (Stark) field to an electrode within the cell modulated the intensity of the wave present at the output of the cell by shifting the resonant frequency of the gas. The modulation of the wave was then detected and amplified. A comparison of the phase and amplitude of the modulation signal with the Stark voltage

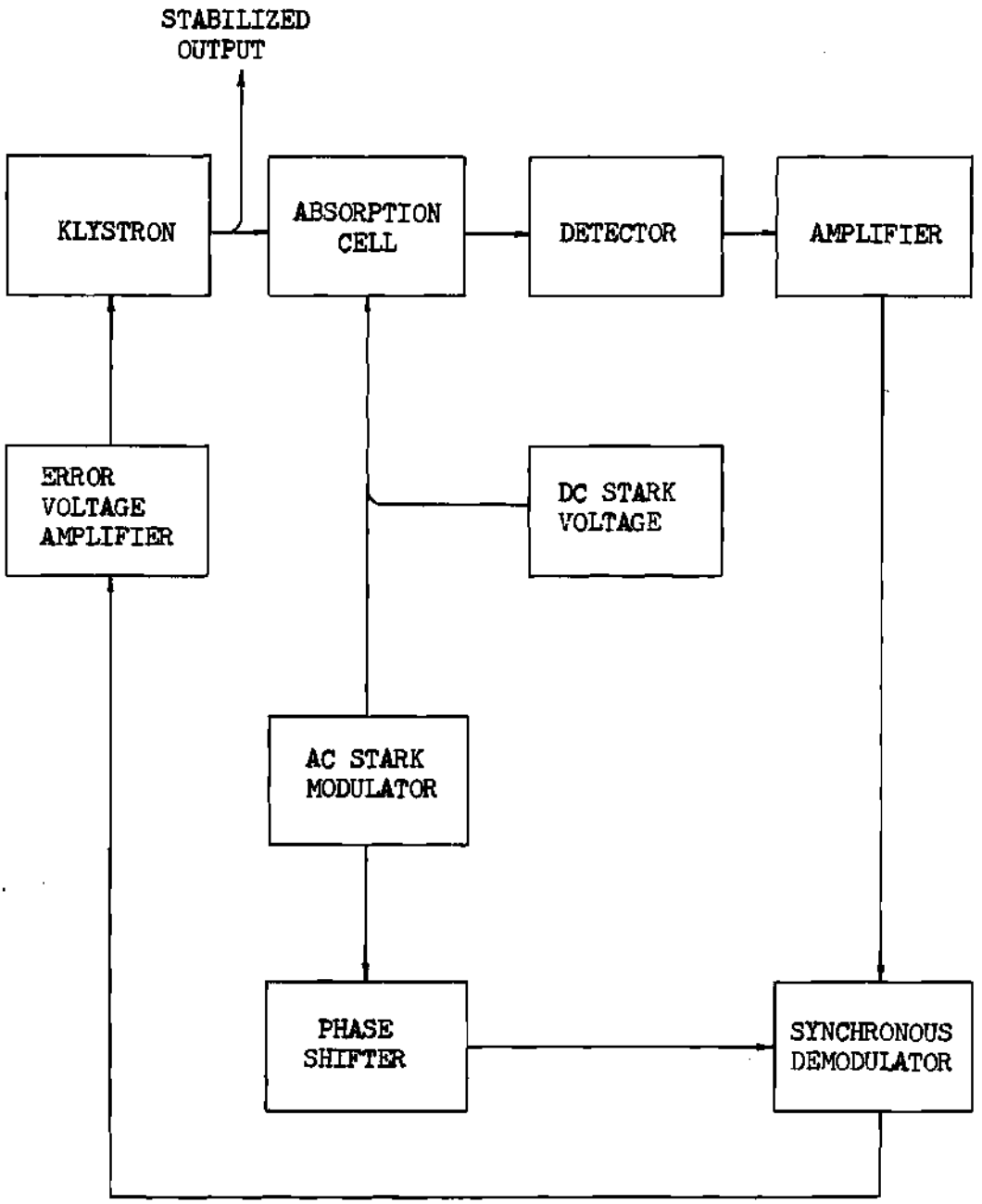

Figure 16. Block Diagram of a Molecular Resonance AFC System

provided a new signal which, after passage through a low-pass amplifier, was used to control the reflector voltage, and hence frequency, of the klystron oscillator.

Signal Oscillator

To demonstrate the stabilization of a millimeter wave source, a Varian VC-710D reflex klystron was selected. This particular device is capable of being tuned over the range of 98 to 104 GHz. Regulated supply voltages for the various klystron elements were supplied by an FXR Universal Klystron Power Supply.

Waveguide Components

A calibrated waveguide attenuator was connected to the klystron to provide a level control and to minimize the return of reflections to the oscillator. Following the attenuator, a cavity wavemeter was inserted in the waveguide for coarse frequency measurements. This device may be used to set the oscillator frequency to within a few hundred megaHertz of the desired molecular resonance frequency. These components are shown in Figure 17.

To allow observation of the oscillator spectrum while operating the molecular resonance AFC system, a "hybrid Tee" was used to obtain a sample of the oscillator output. The output of the wavemeter was connected to the shunt port of the Tee while the series port was terminated in a matched waveguide load. Hence, a 3dB power split was obtained between the two remaining ports. One of these ports was connected via an uncalibrated adjustable attenuator to the absorption cell. The other port was connected via a second uncalibrated adjustable attenuator

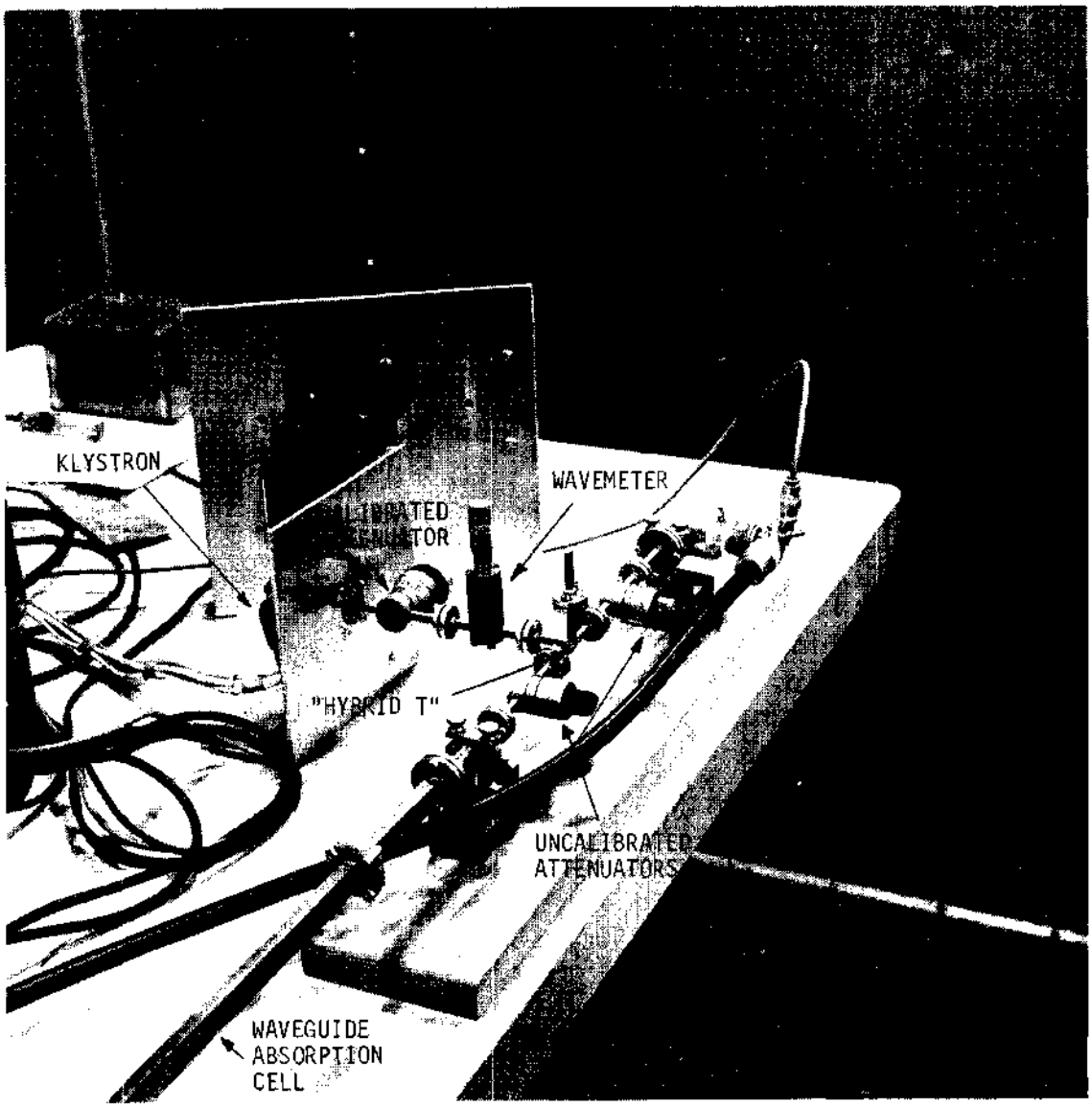

Figure 17. A View of the Millimeter-Wave Components.

to the spectrum analyzer. The attenuators were used to reduce reflections between the absorption cell and the spectrum analyzer input. Each of the above waveguide components are standard W band (75-110 GHz) devices. Spectrum analysis of the oscillator output was performed with a Polarad Model 2992-A Spectrum Analyzer, shown in Figure 18.

Waveguide Absorption Cell

The absorption cell employed in this investigation consists of a four-foot length of standard K-band (18-26.5 GHz) rectangular copper waveguide. The selection of this particular size of waveguide was based primarily on a consideration of mechanical assembly. However, a waveguide of even larger cross-sectional area could have been selected to further decrease the power density within the cell. This would increase the power level at which deleterious power saturation effects (14) first occur. The cross section of the K-band waveguide, though, is sufficiently large that fabrication problems are not excessive, yet small enough to be structurally rigid. Electroformed tapered waveguide transitions were used at each end to transform to W-band waveguide.

The Stark modulation electrode, or septum, consists of a 0.003-inch thick stainless steel (Type 302) ribbon located parallel to the broad walls of the waveguide as shown in Figure 13. Grooved Teflon strips were used to insulate the septum from the waveguide and to support it midway between the broad walls. Electrical connection to the Stark septum was made through a small hole drilled in one of the narrow walls. A steel wire, insulated with a small plastic bushing,

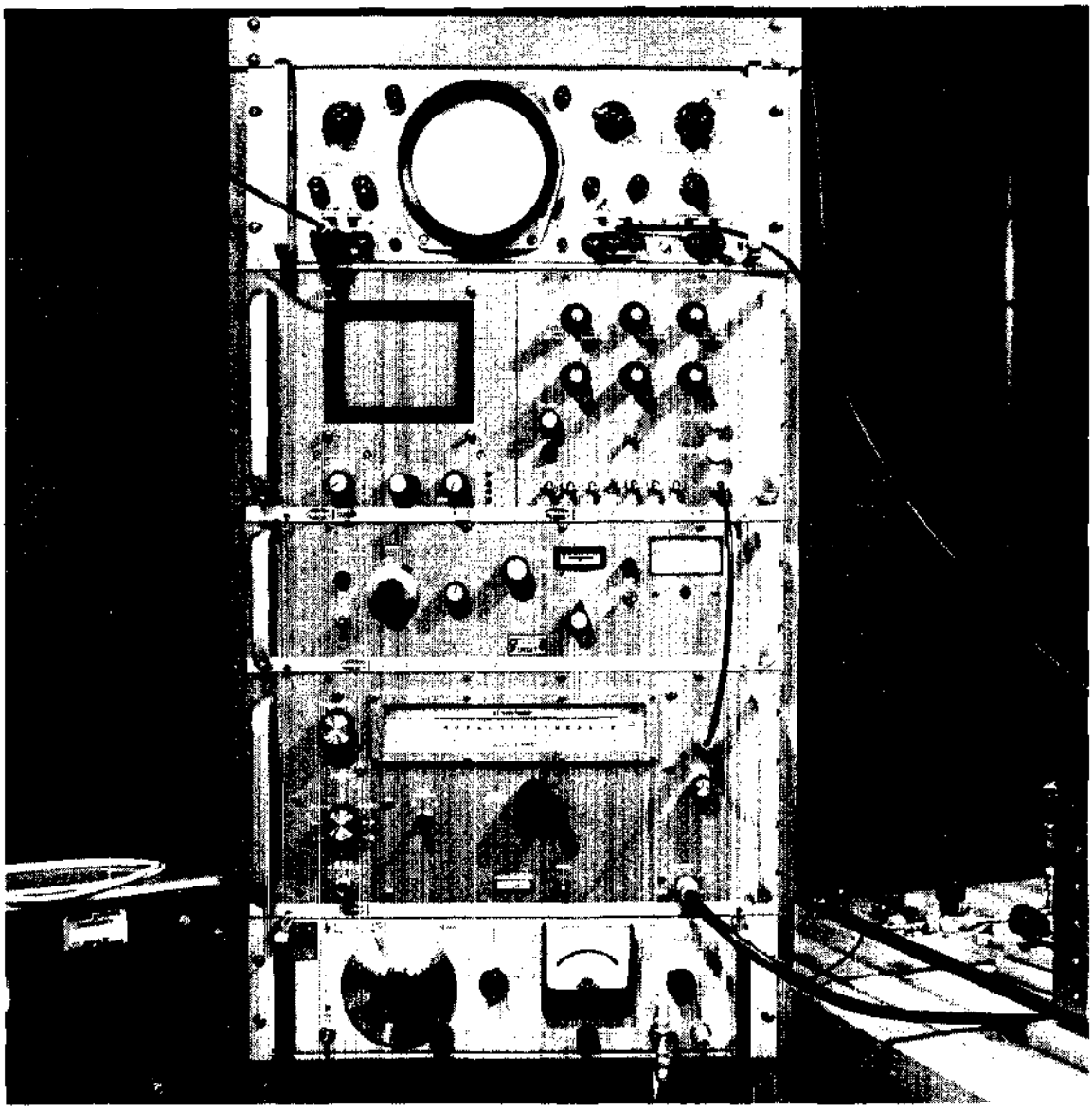

Figure 18. A View of the Spectrum Analyzer.

was placed through the hole and arc welded to the stainless steel. A small, general purpose, capacitor discharge welder was used for this task. Clear Glyptol was used to provide a vacuum-tight seal around the wire and bushing at the point of passage into the waveguide.

To contain the gas within the cell, vacuum-tight windows were used at each end of the absorption cell. They consist of thin (0.003-inch) Mylar film and indium-solder gaskets, cut out to form a seal between the Mylar and the absorption cell waveguide flanges. These windows, shown in Figure 19, provide a low-loss path for the microwave energy, yet enable the gas to be contained within the cell at a low pressure.

Evacuation of the waveguide and subsequent filling with the molecular gas was accomplished through a pair of 0.02-inch holes drilled along the center line of one of the broad walls of the guide. In this region coupling to the electromagnetic fields is minimized and, provided that the dimensions of the holes perpendicular to the direction of power flow in the waveguide are small compared to the wavelength, very little energy will be coupled out through these holes. To allow gas flow into or out of the system, a section of copper tubing was silver-soldered to the waveguide with the drilled holes forming an aperture between the waveguide and the tubing.

A series of bellows-type vacuum valves were arranged so that evacuation and filling can be accomplished through the single piece of tubing connected to the cell. In addition, the valve arrangement provides some control of the volume of gas injected into the system. That is, only the gas trapped between the two valves nearest the

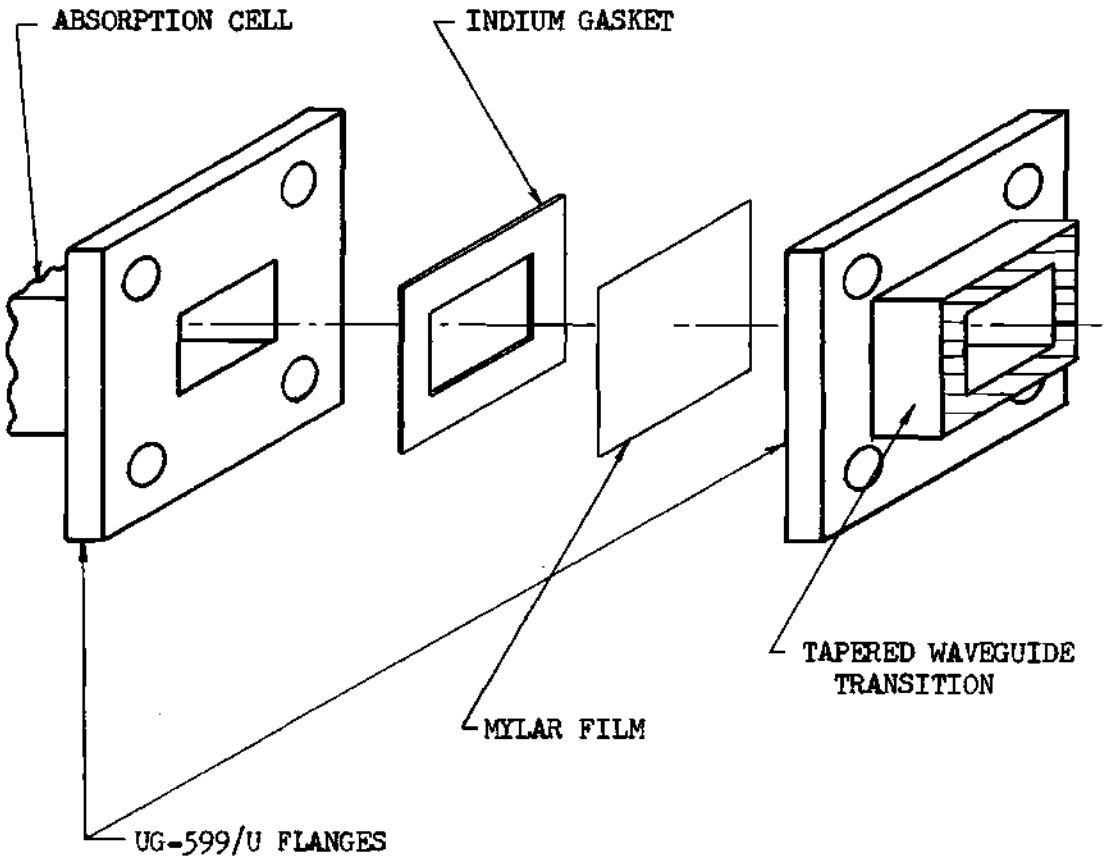

Figure 19. Absorption Cell Vacuum Seals

reservoir is allowed to flow into the cell. A pictorial diagram of the gas system is shown in Figure 20.

Approximate vacuum levels* were determined by means of a Veeco thermocouple gauge. In addition, line width parameters obtained from the literature were used to estimate actual pressures within the cell on the basis of observed line widths.

A two-stage mechanical vacuum pump having a pumping rate of 35 liters per minute was used to evacuate the cell and to adjust the gas pressure after filling. Ultimate vacuums as low as 10^{-4} mmHg may be achieved with this pump. Since this level is substantially lower than levels ordinarily employed in absorption cells, nearly total removal of any air or other gases from the cell prior to filling may be obtained.

The absorption cell insertion loss, $e^{-\alpha_c L}$, required in calculating the discriminator slope, was measured by a substitution method utilizing a calibrated attenuator. The loss of the cell, with the Stark electrode and Teflon supports in place, was observed to be about 7.9dB. Of this amount, 0.7dB was attributed to losses in the two tapered waveguide transitions used at each end of the absorption cell. Hence, an actual absorption cell loss of approximately 7.2dB was noted.

For purposes of comparison, standard perturbational techniques were applied to estimate the losses due to the finite conductivity of the waveguide walls, the stainless steel septum, and the Teflon sup-

---

*No facilities were available for accurately calibrating the vacuum gauge for methyl fluoride.

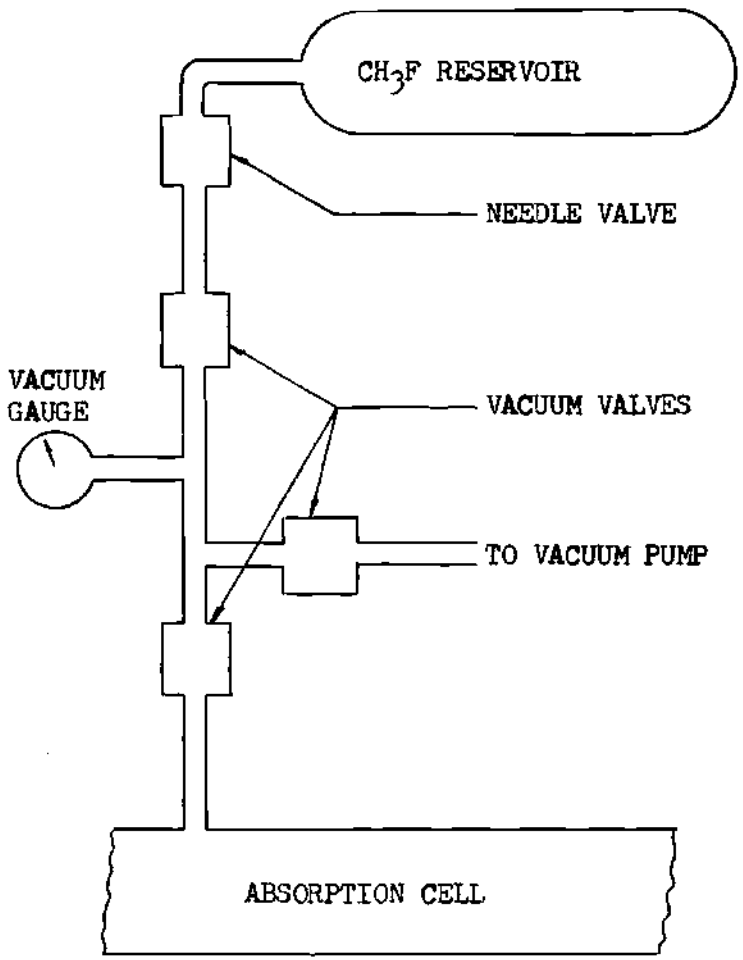

Figure 20. Methyl Fluoride Gas System

porting structure. Assuming a conductivity of 5.7×10^7 mhos per meter and a relative permeability of unity for copper, the procedure outlined by Jordan (21) led to a predicted waveguide loss of 0.5 dB at 100 GHz.

Since the position of the Stark electrode is such that there is no component of $\bar{E}$ tangent to the electrode, the field distribution is unaltered by its presence. In addition, there are no variations in either $\bar{E}$ or $\bar{H}$ as a function of position in a direction normal to the electrode and the broad walls of the waveguide. Therefore, the formulas used to compute losses due to the finite conductivity of the broad walls could also be applied to compute losses due to the Stark septum. Type 302 stainless steel has a resistivity of approximately 40 times that of copper. Hence, the loss due to the internal electrode was predicted to be about 3.0 dB.

A perturbational technique, similar to that proposed by Harrington (22), was employed to estimate the losses introduced by the Teflon supports. The method, outlined in Appendix D, assumes that the Teflon does not substantially perturb the fields, thereby allowing the true dominant mode fields of an empty waveguide to be used in the computations. Moreover, a complex dielectric constant, characterized by a real dielectric constant $2\ \varepsilon_o$ (ε_o - free space permittivity) and a loss factor, $\tan \delta \approx 10^{-3}$ (23), was assumed. Utilizing this approach, a loss of approximately 2.0 dB was predicted as a result of the introduction of the Teflon Stark-electrode supports.

A total absorption cell loss of about 5.5 dB was thus predicted. As noted previously, the measured loss of the absorption cell and its internal structure was about 7.2 dB. On the basis of the relatively

small discrepancy (2.8 dB) between the predicted and observed losses, it may be concluded that predicted values should be satisfactory for use in estimating discriminator slopes.

A major portion of the loss, not accounted for in the theoretical predictions, may be due to the excitation of higher order modes within the absorption cell. The presence of physical discontinuities at each end of the Stark electrode and the Teflon supports may sufficiently perturb the fields, thereby exciting these higher order modes within the absorption cell. These modes, however, cannot propagate in the smaller waveguide leading to the detector. Hence, they may be observed as undesired loss. Some improvement, therefore, could possibly be achieved by tapering the ends of the electrode and the insulating strips, or by inserting tuning elements within the waveguide.

Signal Processing Components

A coaxial-cartridge point-contact silicon crystal detector was used to monitor the amplitude modulation present at the output of the absorption cell due to the alternating Stark field. To obtain maximum sensitivity, it was found that several detectors had to be individually evaluated. Since the semiconductor wafer in such detectors is coupled to the waveguide through a short section of coaxial line, instead of being mounted flush with the walls of the guide, positioning of the device was found to be critical. Both the depth of penetration into the mount and the angular orientation of the cartridge about its axis had a noticeable effect on the sensitivity. Additional tuning of the device was provided by an adjustable waveguide short in shunt with the

the detector. Hence, several adjustments were required to ensure maximum detector output for a given input power level.

As shown in Chapter II, the output of the absorption cell detector may contain all of the harmonics of the modulation frequency. Moreover, the temporal dependence of the frequency separation of the oscillator and the reference introduces sidebands about each harmonic. Since the desired error information is contained in that portion of the spectrum which is centered on the Stark modulation frequency, a tuned amplifier was used to selectively boost the information bearing, or carrier, signal. A synchronous demodulator was then employed to recover the amplitude and phase information on the carrier signal, thereby yielding a low frequency or dc control voltage. A low-pass amplifier provided additional amplification and filtering of the oscillator control voltage.

Selection of the Stark modulation frequency, and hence frequency of the tuned amplifier, was based on a consideration of anticipated linewidths and system noise. To ensure that the molecular resonance frequency can follow the Stark field variations, the modulation frequency must be low. A high modulation frequency, however, is desirable so that the effects of system noise having a spectral amplitude which varies as the reciprocal of frequency are minimized. Moreover, the Stark modulation, or carrier, frequency should be large compared to the system bandwidth so that spurious signals at, or near, the Stark frequency will not be present on the output control voltage.

After consideration of available components, a Stark modulation frequency of 11 kHz, was selected. An amplifier, tuned to this fre-

quency was then constructed. The amplifier, shown schematically in Figure 21, has a voltage gain of 20,000 and a -3 dB bandwidth of approximately 400 Hertz. To minimize loading of the detector, the input impedance of the input transistor Q_1 was increased by reducing the static collector current of Q_1 to approximately 10 microamperes. This resulted in an input impedance of about 50,000 ohms and, at the same time reduced the semiconductor noise to a very low level. Measurements of noise at the amplifier output as a function of resistance placed across the amplifier input indicated that the internally generated noise is approximately the same as that produced by a 600 ohm resistance in series with the base lead of Q_1. Thus, for source impedances much greater than 600 ohms, the amplifier noise will be negligible compared to the noise of the source.

A problem of a highly practical nature arises from the fact that the klystron reflector operates at a potential of about -2500 volts relative to the microwave components and the chassis ground. Hence, some point in the signal path must be broken to provide a large dc offset between the potential of the microwave components and the control voltage circuity. Obviously, a point in the carrier frequency portion of the path is desirable so that either capacitive or inductive coupling may be used to provide continuity of the signal path while allowing a large difference in dc potential.

Tests on standard 6.3 volt, 1.2 ampere filament transformers indicated satisfactory performance at 11 kHz and yet are capable of providing the necessary voltage isolation. Moreover, a voltage gain of about 18 was obtained. Two such transformers were employed in the

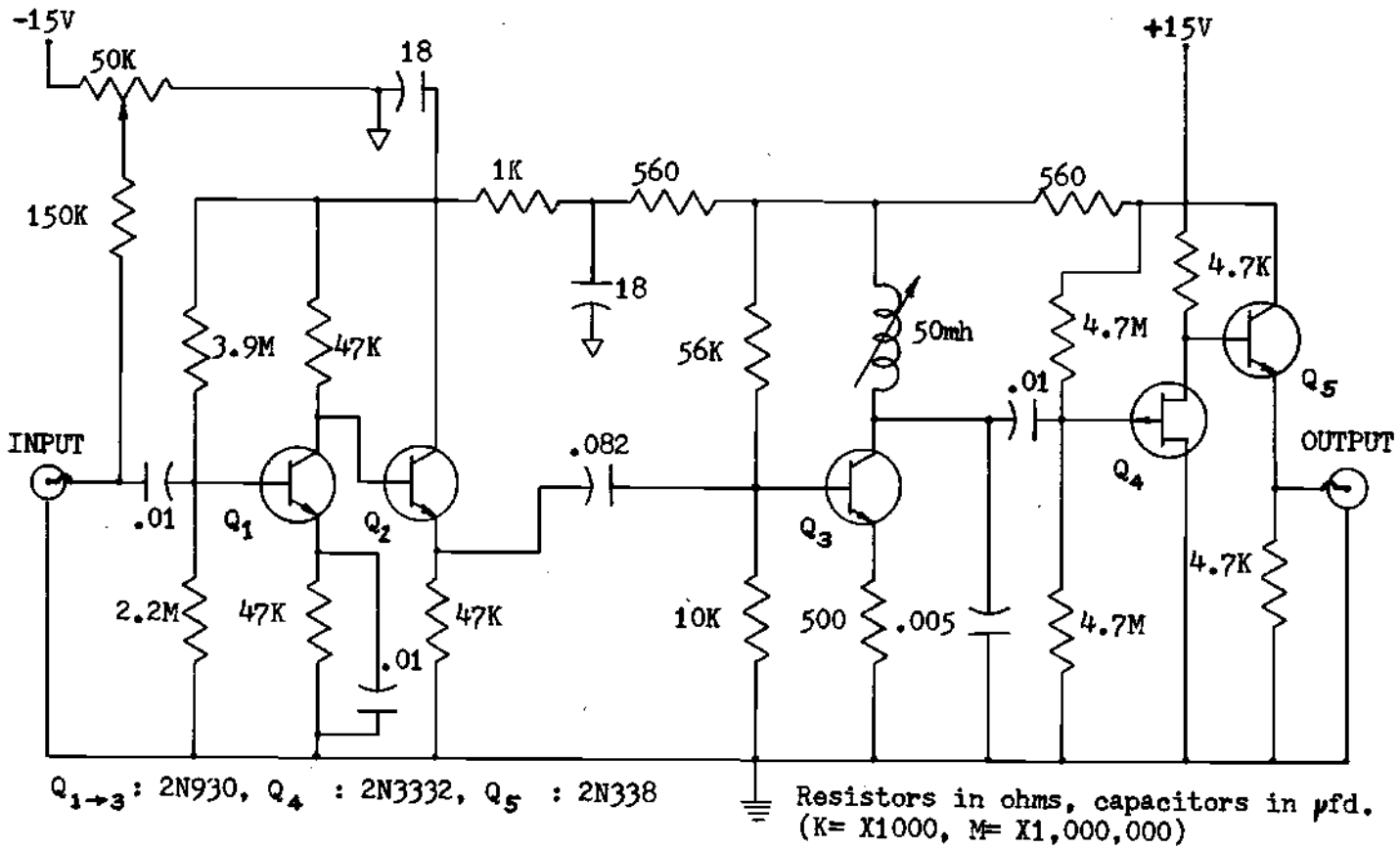

Figure 21. Tuned Amplifier Schematic Diagram

system. One was connected between the tuned amplifier and the synchronous demodulator while the second was used to supply the Stark frequency reference to the demodulator. Hence, the demodulator and low-pass control voltage amplifier are allowed to float at the reflector potential.

A schematic diagram of the demodulator circuit, including the low-pass amplifier to boost the control voltage, is presented in Figure 22. This circuit is mounted in a small aluminum box which is insulated from the remainder of the microwave components. Inputs for both the amplified signal from the detector and the Stark modulation reference are provided via BNC connectors. The output to the klystron reflector and power supply is connected via two UHF-type coaxial connectors. Power for the active circuits on the phase comparison unit may be obtained either from two 15-volt batteries or from an ac operated supply.

The demodulator provides an output voltage which is proportional to the amplitude of the 11 kHz signal from the tuned amplifier and whose polarity is fixed by the phase relationship between the input signal and the reference obtained from the Stark modulation source. Coincidence of the klystron and the molecular resonance frequencies is evidenced by a null in this output voltage. When the klystron frequency is below the resonance of the gas, the 11 kHz signal from the detector will be in phase with the Stark voltage. Conversely, the 11 kHz signal will be 180 degrees out of phase with the modulating signal when the oscillator is tuned above the resonant frequency of the gas. Thus, a dc voltage is produced which is proportional to C_1 of Equation (2-12). Further

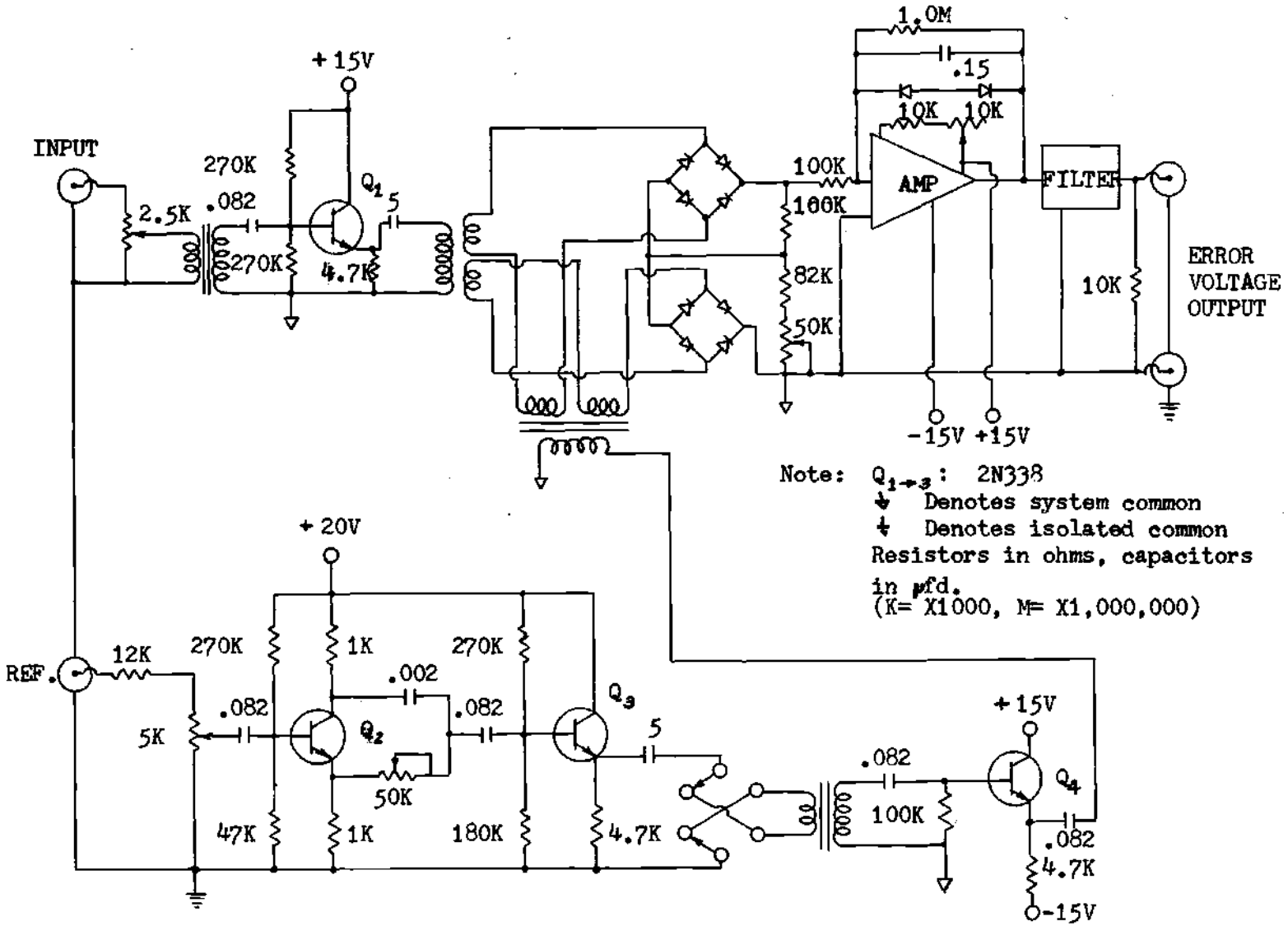

Figure 22. Synchronous Demodulator Schematic Diagram

amplification and filtering was obtained with an encapsulated operational amplifier whose feedback was adjusted according to the desired gain and low-pass bandwidth. Interconnections between the tuned amplifier, the synchronous demodulator, and the Stark modulator are shown in Figure 23.

A Hewlett-Packard 651A Oscillator was used to supply the 11 kHz Stark modulation voltage and the reference for the synchronous demodulator unit. A simple RC phase shifter was inserted in the line from the 651A oscillator and the isolation transformer leading to the input of the phase comparison unit to provide compensation for phase shift in the tuned amplifier.

The dc component of the Stark voltage was supplied by a Hewlett-Packard 721A Power Supply. For the methyl fluoride system a dc voltage of approximately 10 volts was used. The selection of this dc Stark voltage was based on a consideration of the influence of undesired absorption lines. For the $J = 1 \rightarrow 2$ transition of methyl fluoride, a single undesired line is present. Hence, recalling (2-16), it may be shown that the shift in the position of the discriminator null from the center of the desired line is given by

$$\left[1 + \left(\frac{\beta}{\Delta f}\right)^2\right]^{\frac{3}{2}} \left(\frac{\delta f_2}{\Delta f}\right)^{-3} \Delta f$$

If the magnitude of β is assumed to be optimized to $\Delta f/\sqrt{2}$, for maximum discriminator slope, the observed null shift will be $1.83 \left(\frac{\delta f_2}{\Delta f}\right)^{-3} \Delta f$. Furthermore, the separation δf_2 of the peak of the undesired line and

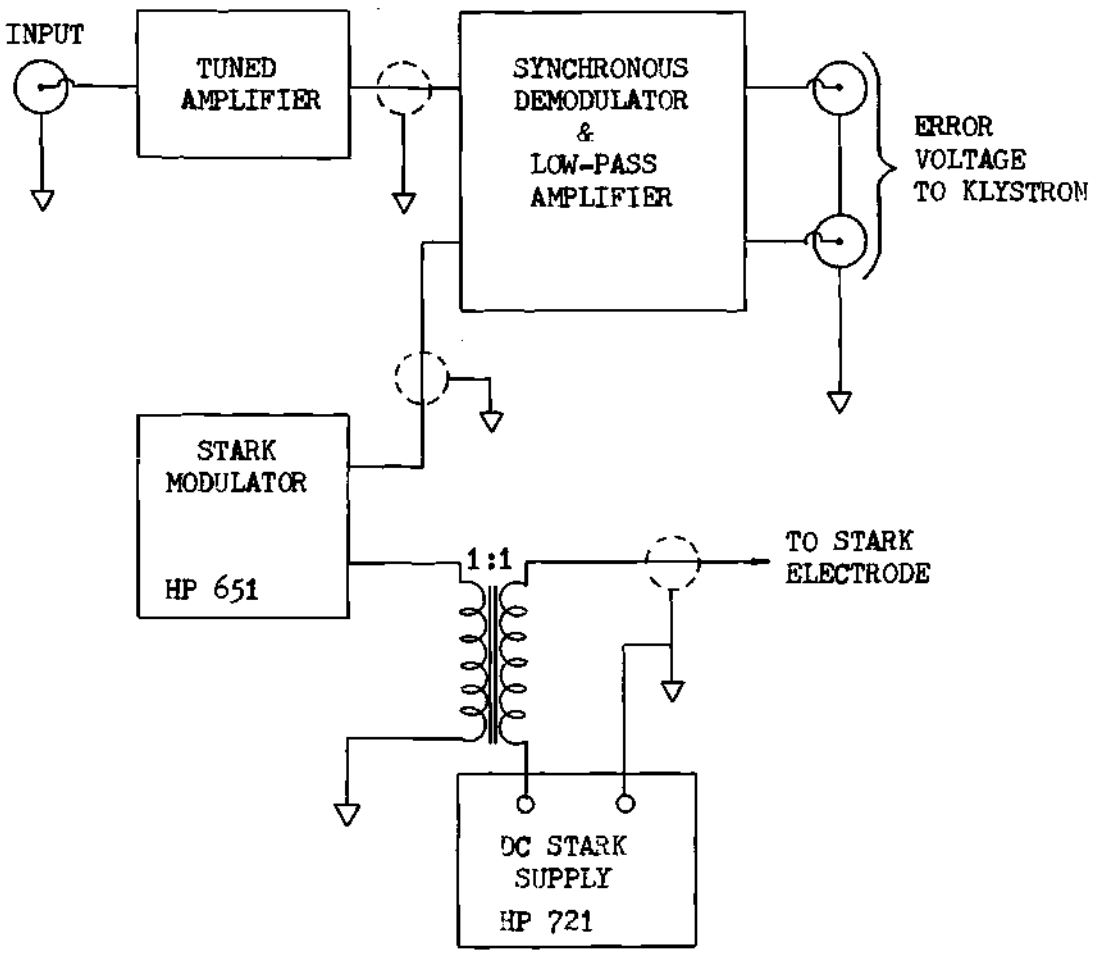

Figure 23. Interconnections of Stark Field Sources, Tuned Amplifier and Synchronous Demodulator

the desired line is twice the shift of either line from the zero field position. Thus if the dc Stark field shifts each line 5 Δf, the null will move less than 0.2 per cent of Δf. Increasing the shift to 10 Δf reduces the null shift to less than 0.025 per cent of Δf. From (4-5), the predicted separation of the desired and undesired lines is 2.8 V_{dc} x 10^6 Hertz. In terms of the dc Stark voltage V_{dc}, the shift in the discriminator null is approximately $8(V_{dc})^{-3}(\Delta f)^4 \times 10^{-20}$. For a dc Stark voltage at 10 volts and a linewidth, Δf, of 2×10^6 Hz, the null shift from the center of the desired line is less than 1.5 kHz. The center of the desired line, though, is about 24 MHz from the line center in the absence of the dc Stark field.

Preliminary Test Configuration

To facilitate testing of the system, jacks were provided to monitor the outputs of the tuned amplifier and the phase shifter. When connected to an oscilloscope as shown in Figure 24, the discriminator action of the molecular gas can be readily observed by the change in the slope of the oscilloscope trace as the oscillator frequency or dc Stark voltage, and hence reference frequency, is varied. When the oscillator and reference frequencies coincide, the Stark modulation component of the absorption cell output is zero. Thus zero voltage will be applied to the vertical deflection system of the oscilloscope and a horizontal trace will be observed. If either the oscillator frequency or the reference frequency is changed, the oscilloscope trace will tilt according to the magnitude and direction of change.

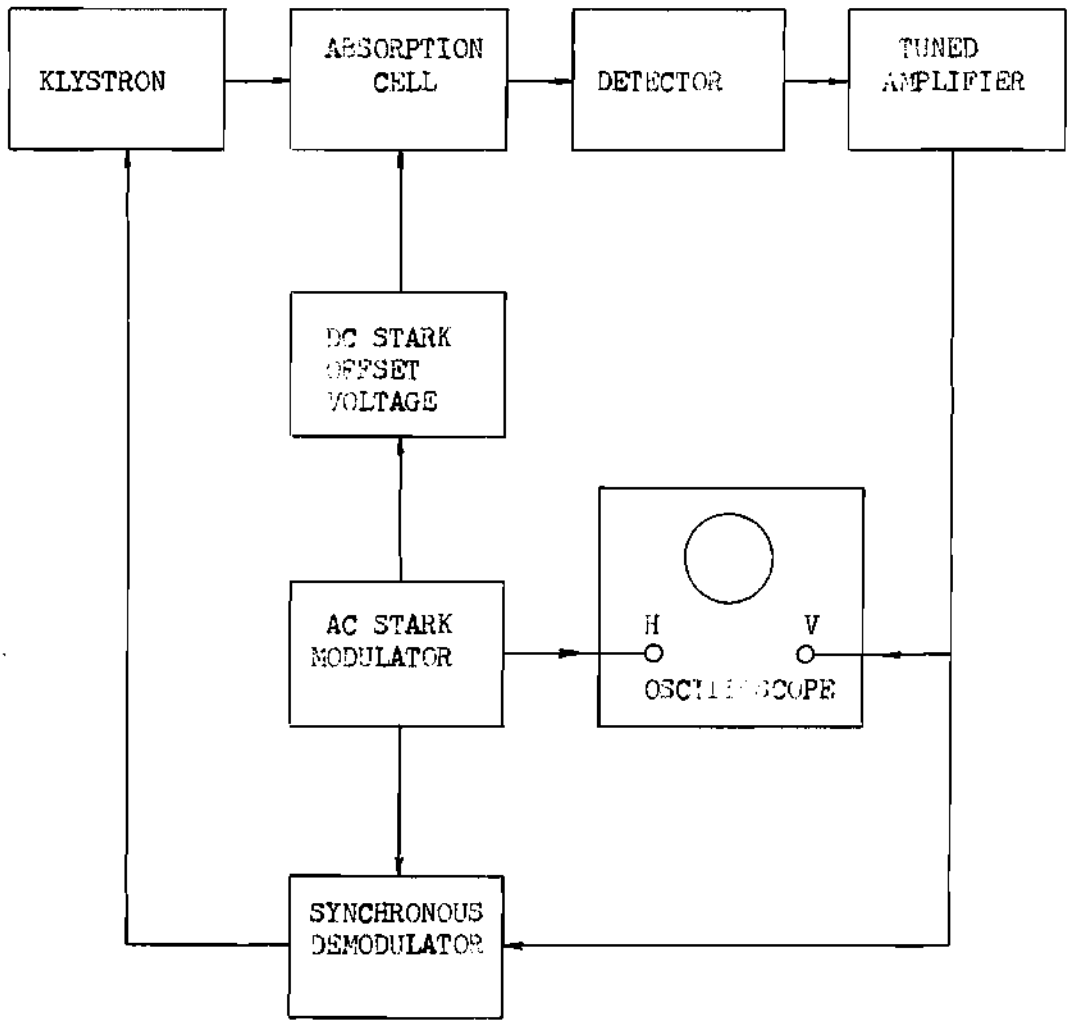

Figure 24. Preliminary Test Configuration for Observation of Molecular Discriminator Action

Calculated Loop Gain

To estimate the performance expected from the methyl fluoride AFC system, the loop gain, $1 + AK_D K_m$, was computed. For this purpose the following parameters were assumed:

$$\gamma = 10^2 \text{ volts per watt}$$

$$P_i = 2 \times 10^{-3} \text{ watts}$$

$$e^{-\alpha_c L} = 0.16 \text{ (-7.9 dB)}$$

$$\alpha_o = 0.125 \times 10^{-3} \text{ cm}^{-1}$$

$$L = 122 \text{ cm}$$

$$\Delta f = 2 \times 10^6 \text{ Hz}$$

It was further assumed that the amplitude of the alternating Stark voltage was adjusted so that β was approximately $\Delta f/\sqrt{2}$ for maximum discriminator slope. Hence from (2-18) it was shown that $K_D \approx 1.3 \times 10^{-10}$

The amplifiers and transformers employed in the methyl fluoride stabilization system provided a maximum voltage gain of slightly more than 2×10^6. This gain figure may be separated into the following: 2×10^4 for the tuned amplifier, approximately 18 for the isolation-

---

*Theoretically, Δf could be optimized to further increase K_D to 2.6×10^{-10} according to (3-6). However, there appeared to be contamination of the methyl fluoride, which at lower pressures, broadened the absorption line and reduced the intensity. Thus, the full benefit of a reduced linewidth could not be achieved.

coupling transformer, and 6 for the synchronous demodulator-low pass amplifier combination. Hence, for a power level of two milliwatts, and an observed klystron modulation sensitivity of 4.5×10^6 Hz/volt, the predicted loop gain was about 1.2×10^3.

Evaluation of the Methyl Fluoride System

To evaluate the performance of the methyl fluoride AFC system, a comparison of open- and closed-loop drift was made. In addition, the influence of noise within the system was observed by means of a spectrum analyzer.

Measurement of the closed-loop klystron frequency drift was accomplished by calibrating the output level of the tuned amplifier as a function of oscillator frequency. The spectrum analyzer was used to determine the frequency shift of the klystron, with the loop closed, as the reflector voltage was slowly varied. Observation of the tuned amplifier output at various settings of the oscillator frequency enabled calibration of the discriminator slope. Since an ac voltmeter was used to monitor the modulation frequency output, the klystron frequency had to be tuned away from the null of the discriminator for unambiguous measurement of drift in either direction about the present frequency. A plot of the closed loop variations thus obtained, is presented in Figure 25. Over a period of two hours, the total drift did not exceed 12 kHz from the preset frequency. On the basis of the open-loop drift (Figures 14 and 15) and the predicted loop gain ($\approx$ 1200) this might seem excessive. However, the position of the discriminator null, which depends on the dc Stark voltage, may have shifted, thereby

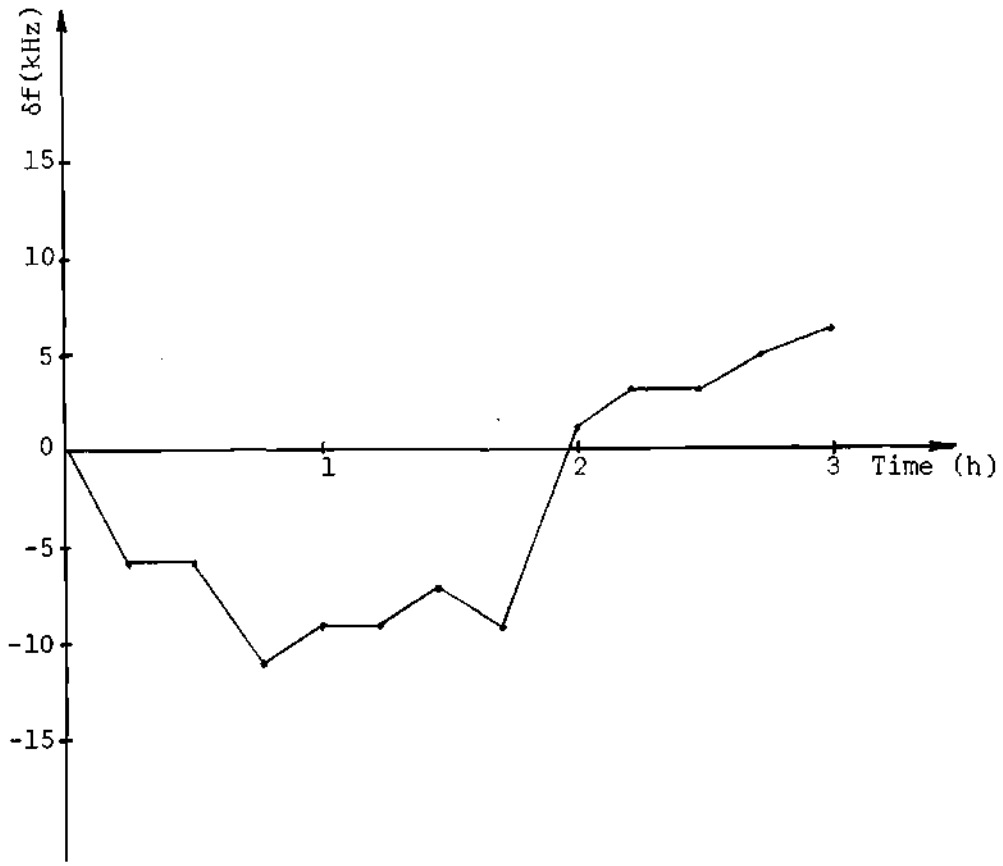

Figure 25. Observed Closed Loop Drift

introducing the possibility of erroneous observations. The Stark shift is 1.4 mHz per volt, thus allowing a one kiloHertz shift in the reference frequency for each 0.7 millivolt change in the dc Stark supply. Since the supply used for this voltage has a regulation of 15 millivolts for

10 per cent changes in line voltage, there may be some error in the observed 12 kHz drift.

An additional check on the system performance was obtained by manually varying the klystron reflector voltage over a ±10 volt range (the limits of the output swing of the low-pass amplifier) while observing the frequency on the spectrum analyzer. This change in voltage corresponds to an open-loop frequency shift of about 90 MHz. Under closed-loop conditions, however, the stabilized oscillator frequency changed less than 100 kHz for the same reflector voltage variation. Therefore the measured loop gain, the ratio of open-loop deviations to closed-loop deviation, appears to be in excess of 900, and in fair agreement with the theoretically predicted value of 1200.

The spectrum analyzer was also used to monitor the rapid variations of the closed loop frequency. The observed spectrum consisted of the stabilized signal and sidebands produced by noise. With a loop bandwidth of one Hertz, the spectral width occupied by the noise sidebands was about 60 kHz. Hence, a short-term stability of no better than approximately 3 parts in 10^7 can be expected.

The observed spectral width, on the basis of Equation (3-8), indicates that an effective noise voltage of about 4 μV was present at the input of the tuned amplifier. However, for a detector exhibiting only thermal noise, the noise temperature ratio, t, in (3-7) is unity. If the ambient temperature is assumed to be 300°K and the video resistance is 5000 ohms, a noise voltage of only 0.01 μV is predicted for an effective noise bandwidth of $\pi/2$ Hz (-3 dB bandwidth = 1 Hz). Since the observed noise voltage is greater than two orders of magnitude

more than that predicted on the basis of thermal noise alone, a noise temperature ratio in excess of 10^4 is indicated. This value, however, is not in disagreement with the noise ratios observed in other systems, such as CW Doppler radars, where the carrier is used as a local oscillator to demodulate the information bearing signal. In the Stark modulation system a similar demodulation process, in which the sidebands produced by the Stark field are mixed with the signal frequency at the absorption cell detector, exists. This similarity to the demodulation process used in the CW Doppler radar therefore provides a suitable comparison.

Thus, it may be concluded from the above discussion that an automatic frequency control system, based on a molecular resonance, may readily provide at least two orders of magnitude improvement in the stability of a 100 GHz klystron oscillator. Furthermore, the proposed method can be easily adapted for use at many other frequencies merely by selecting a different gas and by making appropriate adjustments to the Stark voltage and amplifier gain.

CHAPTER VI

CONCLUSIONS AND RECOMMENDATIONS

The existence of numerous energy absorbing molecular resonances throughout the microwave and millimeter-wave regions of the electromagnetic spectrum has been demonstrated by several investigators, principally in the area of microwave spectroscopy. To explain the spectral shape of the absorption lines observed by the microwave spectroscopists, Van Vleck and Weisskopf (6) developed a theory of gaseous absorption due to molecular resonances. Utilizing the theoretically predicted line shapes, the author demonstrated that these resonances, when modulated by application of the Stark effect, may be used as frequency discriminators.

A feedback control system, based on a "molecular" discriminator employing methyl fluoride gas, was constructed. Observed data demonstrated that a substantial improvement in the long-term stability of a 100 GHz reflex klystron oscillator was obtained. To the author's knowledge, this is the first time that a Stark-shifted molecular resonance has been used to stabilize the frequency of a millimeter-wave oscillator. On the basis of data found in the literature (20,24), the characteristics of the methyl fluoride molecule may be assumed to be representative of several other molecules, each having known resonances in the millimeter region of the spectrum. Hence, it is therefore concluded that the proposed system could be employed at other frequencies

without sacrifice of performance.

The values of detector sensitivity observed during the course of this investigation appear to be disproportionately low. If the sensitivities cited by Uhlir (16) and Whitford (17) may be assumed to be typical, the loop gain, for a fixed amplifier gain, could then be expected to be at least an order of magnitude greater than actually observed in the laboratory. Thus, further investigation of crystals for use in detecting the modulation present at the absorption cell output is warranted.

The long-term stability obtained with the methyl fluoride stabilization system compares favorably with the quoted stability of several commercial frequency control units. Generally these systems are based on a quartz crystal oscillator reference and employ phase-lock techniques. Thus, no steady state errors can exist between the reference frequency and the stabilized output frequency. Hence, the overall system stability is determined by the stability of the crystal oscillator reference. The molecular discriminator, on the other hand, is a frequency-lock system. In such a system, the closed-loop stability is a function of the open-loop drift of the signal oscillator since steady state errors between the controlled oscillator frequency and the stable molecular resonance frequency may exist. In the laboratory system, the loop gain was sufficiently high so that existing steady state errors were reduced to an acceptable level.

The system reported here appears to be a satisfactory approach to the problem of frequency control at millimeter-wavelengths. Certain limitations, however, should be pointed out. Unlike crystal oscillator

referenced systems, stabilization may be achieved only near a natural molecular resonance frequency. Recent developments in microwave single-sideband techniques may enable the molecular discriminator stabilization system to be used at frequencies up to several hundreds of megaHertz from the molecular resonances. In such systems, the oscillator frequency could be offset a fixed amount by modulating the signal oscillator with the output of a crystal controlled oscillator, the offset frequency being compared with, and stabilized by, the molecular reference. The stability of the signal oscillator will then be dependent on both the feedback system and the crystal oscillator used to provide the offset frequency.

Some difficulty might also be encountered in obtaining satisfactory detector sensitivities at frequencies above 100 GHz. Uhlir (16), though, presents data on a crystal detector designed for operation in the vicinity of 150 GHz. In addition, TRG, Inc. has recently announced development of bolometer detectors having a resistance sensitivity of 120 ohms per milliwatt of power with a bias current of 0.5 ma. These devices are intended for use at frequencies up to 220 GHz. Thus, voltage sensitivities of 60 volts per watt should be readily attainable in the millimeter region. Moreover, their time constants are such that Stark modulation frequencies of 10 kiloHertz or higher may be employed. In contrast to the biased crystal detectors, the bolometers exhibit no 1/f semiconductor noise. Hence, wider bandwidths could be employed in the amplifier portion of the feedback loop with a resulting improvement in short-term stability.

It is recommended, therefore, that millimeter-wave single-sideband techniques be investigated in order that increased flexibility may be incorporated into the system. Also, new bolometers, as they become available, should be investigated. Finally, the inclusion of a servo-motor to provide mechanical tuning of the oscillator should be investigated as a means of further counteracting long-term drift. The same techniques employed in this research could also be used to advantage in an investigation of random fluctuations of the propagation delay of a millimeter-wave signal over multiple atmospheric paths.

APPENDICES

APPENDIX A

THE QUANTIZED ENERGY LEVELS OF A SYMMETRIC-TOP MOLECULE

The quantized rotational energy levels for a rigid rotating molecule may be determined by solving the wave equation of the system, subject to certain boundary conditions, as shown by Reiche and Rademacher (2). In the following paragraphs, a review of their work is presented.

Let it be assumed that the total kinetic energy of the molecule may be represented by

$$T = \sum_i \sum_k A_{ik} p_i p_k \qquad \text{(A-1)}$$

where p_i and p_k are components of the angular momentum in the directions of the ith and kth coordinates, respectively, and A_{ik} is the coefficient of the cross-product $p_i p_k$. In a three-dimensional system, both i and k may take on the values 1, 2, and 3. Moreover, it is assumed that the molecule possesses no translational or potential energy.

Having obtained the above coefficients, A_{ik}, Schrödinger's steady state wave equation (3),

$$\hbar^2 A^{\frac{1}{2}} \sum_k \frac{\partial}{\partial q_k} \left(A^{-\frac{1}{2}} \sum_i A_{ik} \frac{\partial \psi}{\partial q_i} \right) + \varepsilon \psi = 0 \qquad \text{(A-2)}$$

may be employed to determine the allowable energy levels ε. In (A-2)

$\hbar = \frac{h}{2\pi}$, q_k is the kth coordinate of the system, and A is the value of the determinant of the coefficients A_{ik}. In the case of a rigid symmetric-top molecule, the orientation and motion of the molecule is most conveniently expressed in terms of the Euler angles, θ, χ, and ϕ. Thus, it is assumed that a rectangular coordinate system x, y, z fixed relative to the molecule may be obtained from a series of simple rotations of a space-fixed coordinate system X, Y, Z. If z is considered to be in the direction of the molecular axis of highest symmetry, the position of the body is then specified from an initial position in which the two systems coincide. Hence, the body is first rotated through an angle ϕ about the Z axis, then about the x axis through an angle θ, and finally through an angle χ about the z axis. The coordinates of interest are, therefore, $q_1 = \theta$, $q_2 = \chi$, and $q_3 = \phi$.

In this coordinate system the total kinetic energy is given by,

$$T = \frac{1}{2I_A} p_\theta^2 + \frac{1}{2}\left(\frac{1}{I_c} + \frac{\cos^2\theta}{I_A \sin^2\theta}\right) p_\chi^2 + \frac{1}{2I_A \sin^2\theta} p_\phi^2 - \frac{\cos\theta}{I_A \sin^2\theta} p_\phi p_\chi \quad \text{(A-3)}$$

where I_A is the moment of inertia about either the x or y axes and I_c is the moment of inertia about the z axis.

The coefficients A_{ik} may be obtained from (A-3). Insertion of these terms into (A-2) yields the desired wave equation after some algebraic manipulations,

$$\frac{\partial^2\psi}{\partial\theta^2} + \frac{\cos\theta}{\sin\theta}\frac{\partial\psi}{\partial\theta} + \left[\frac{I_A}{I_c} + \frac{\cos^2\theta}{\sin^2\theta}\right]\frac{\partial^2\psi}{\partial\chi^2} + \frac{1}{\sin^2\theta}\frac{\partial^2\psi}{\partial\phi^2} - \frac{2\cos\theta}{\sin^2\theta}\frac{\partial^2\psi}{\partial\phi\partial\chi} + \frac{2I_A\varepsilon}{h^2}\psi = 0 \quad \text{(A-4)}$$

The solution of (A-4) is generally obtained by the method of separation of variables. Hence, it is postulated that $\psi = \Theta(\theta)e^{j(M\phi+K\chi)}$ where $\Theta(\theta)$ represents the functional dependence of ψ on θ, $j = \sqrt{-1}$ and M and K are integers. The resulting equation for Θ is

$$\frac{\Theta''}{\Theta} + \frac{\cos\theta}{\sin\theta}\frac{\Theta'}{\Theta} + \frac{-M^2}{\sin^2\theta} - K^2\left[\frac{I_A}{I_c} + \frac{\cos^2\theta}{\sin^2\theta}\right] + 2MK\frac{\cos\theta}{\sin\theta} + \frac{2I_A\epsilon}{h^2} = 0 \qquad \text{(A-5)}$$

where the prime indicates a derivative with respect to θ.

Further simplification may be achieved through the substitution $y = \cos\theta$. Thus, (A-5) is transformed to

$$(1 - y^2)^2\frac{d^2u}{dy^2} - 2y(1 - y^2)\frac{du}{dy} + [f + ey - \lambda y^2]u = 0 \qquad \text{(A-6)}$$

where Θ is replaced by u and

$$f = \frac{2I_A\epsilon}{h^2} - \frac{I_A}{I_c}K^2 - M^2 = \lambda - (M^2 + K^2)$$

$$\theta = 2MK$$

$$\lambda = \frac{2I_A\epsilon}{h^2} - \frac{I_A}{I_c}K^2 + K^2$$

Now, letting $y = 1 - 2t$, (A-6) is further transformed to

$$4t^2(1-t^2)\frac{d^2u}{dt^2} - 4T(1-2t)(1-t)\frac{du}{dt} - [(\lambda - e - f) + (2e - 4\lambda)t + 4\lambda t^2]u = 0 \qquad \text{(A-7)}$$

Note, however, that $\lambda - e - f = (M - K)^2$ and $2e = (M + K)^2 - (M - K)^2$. Hence, letting $|M + K| = s \geq 0$ and $|M - K| = d \geq 0$, we obtain

$$\frac{d}{dt}\left[t(1 - t)\frac{du}{dt}\right] - \frac{d^2 + (s^2 - d^2)t}{4t(1 - t)}u + \lambda u = 0 \qquad \text{(A-8)}$$

Replacing u by $wt^{\frac{d}{2}}(1 - t)^{\frac{s}{2}}$ in (A-8) yields

$$t(1-t)\frac{d^2w}{dt^2} + [(1+d) - (2+d+s)t]\frac{dw}{dt} - \left[\left(\frac{d+s}{2}\right)\left(\frac{d+s}{2} + 1\right) - \lambda\right]w = 0 \qquad \text{(A-9)}$$

Equation (A-9) may be shown to be the form of Gauss' Hypergeometric Equation if we let $\gamma = 1 + d$, $\alpha + \beta = 1 + d + s$, and $\left(\frac{d+s}{2}\right)\left(\frac{d+s}{2} + 1\right) - \lambda = \alpha\beta$,

$$t(1 - t)\frac{d^2w}{dt^2} + [\gamma - (\alpha + \beta + 1)t]\frac{dw}{dt} - \alpha\beta w = 0 \qquad \text{(A-10)}$$

The solution of (A-10), known as a hypergeometric function, is a power series in t. For the solution to be a satisfactory normalizable wave function, though, the series must terminate and become a polynomial. Thus it is required that $\lambda = \left(\frac{d+s}{2} + n\right)\left(\frac{d+s}{2} + n + 1\right)$ where $n = 0,1,2,\cdots$ and n is the degree of the resulting polynomial.

Moreover, it may be shown that $\frac{d + s}{2}$ is an integer, m^*, and is numerically equal to the greater of the two values $|K|$ and $|M|$. Hence, $\lambda = (m^* + n)(m^* + n + 1) = J(J + 1)$ where J is also an integer. In addition, the following inequalities must hold: $|M| \leq J$ and $|K| \leq J$. The resulting expression for the allowable energy levels (J,K,M) is,

$$\varepsilon(J,K,M) = \frac{J(J+1)\hbar^2}{2I_A} + K^2\left(\frac{\hbar^2}{2I_c} - \frac{\hbar^2}{2I_A}\right) \qquad \text{(A-11)}$$

A physical interpretation of the numbers J, K, and M may be derived from an analysis of the energy equation of a classical rotating top. That is, the total energy of rotation is given by

$$\varepsilon = \frac{P_x^2}{2I_x} + \frac{P_y^2}{2I_y} + \frac{P_z^2}{2I_z}$$

where P_x, P_y, and P_z are the components of angular momentum about each of the coordinate axes x, y, z. In addition, $P_x^2 + P_y^2 + P_z^2 = P^2$, where P^2 is the square of the total angular momentum. In the case of a symmetric-top molecule, the moments of inertia I_x and I_y are equal and are generally designated I_A, while I_z is represented by I_c. Thus,

$$\varepsilon = \frac{P^2 - P_z^2}{2I_A} + \frac{P_z^2}{2I_c} \qquad \text{(A-12)}$$

$$= \frac{P^2}{2I_A} + P_z^2\left(\frac{1}{2I_c} - \frac{1}{2I_A}\right)$$

and the quantity $J(J+1)\hbar^2$ may be interpreted as the square of the total angular momentum. On the other hand, the term $K^2\hbar^2$ may be interpreted as the square of the component of momentum about the axis of highest symmetry. Furthermore, since J and K may assume only integer values, the energy is said to be quantized.

Finally, the similarity of the wave function dependence on χ

and ϕ indicates that $M^2\hbar^2$ may be interpreted as the square of the component of angular momentum about the space-fixed Z axis. Hence, the state of rotational energy of the molecule is completely specified by the three "quantum numbers" J, K, and M.

It may also be shown that the probability of a transition from one energy level to another will be nonzero only if

$$\Delta J = 0, \pm 1; \qquad \Delta K = 0; \qquad \text{and} \qquad \Delta M = 0, \pm 1$$

In the absence of external fields the last rule may be ignored. Rotational absorption spectra result for $\Delta J = +1$, emission spectra for $\Delta J = -1$, and inversion spectra for $\Delta J = 0$. Thus, applying Bohr's postulate, the absorption frequency f for a transition $J \rightarrow J + 1$, is given by

$$f_o = \frac{\left[\frac{(J+1)(J+2)\hbar^2}{2I_A} + K^2\left(\frac{\hbar^2}{2I_A} - \frac{\hbar^2}{2I_c}\right)\right] - \left[\frac{J(J+1)\hbar^2}{2I_A} + K^2\left(\frac{\hbar^2}{2I_A} - \frac{\hbar^2}{2I_c}\right)\right]}{h}$$

$$= 2B(J + 1) \qquad \text{(A-14)}$$

where $B = \frac{h}{8\pi^2 I_A}$ is a constant for a particular molecule.

Having specified the total angular momentum $J(J + 1)\hbar$ and its components, $K\hbar$ and $M\hbar$, one may determine appropriate coefficients which normalize the wave functions ψ of (A-4) so that $\int_\tau \psi_{JKM}\,\psi^*_{JKM} d\tau = 1$, when τ is the entire coordinate space. These wave functions may then

be used to predict the effect of small perturbations of the system energy as will be shown in Appendix C.

APPENDIX B

THE VAN-VLECK-WEISSKOPF LINE SHAPE

A theory of resonant absorption has been developed by Van Vleck and Weisskopf (6) which yields predicted line shapes that agree with experimentally observed microwave molecular resonance spectra. Moreover, the Van Vleck-Weisskopf theory reduces to the nonresonant case examined by Debye (25) when the rotational energy of the molecule is negligible. A summary of their derivations is presented by Townes and Schawlow (26) and will be reproduced here for completeness.

The derivation of an expression for the absorption coefficient of a rotating, polarized molecule is based upon the assumption that the molecule is in thermal equilibrium with the surrounding electromagnetic field and that the phases of motion follow a Boltzmann distribution. In addition, the rotational motion may be resolved into orthogonal linear vibrations. Hence, only a single linear oscillator need be examined.

From the classical equation of motion for a linear oscillator, the complex dielectric constant of a molecular gas may be determined. For an oscillator whose mass is $\underline{m}$ and charge is $\underline{e}$, the equation of motion is of the form,

$$\ddot{x} + \omega_o^2 x = \frac{eE}{m} \cos\omega t \qquad \text{(B-1)}$$

where $\omega_o (=2\pi f_o)$ is the angular frequency of the oscillator and $\omega (=2\pi f)$ is that of the applied electric field. The intensity of the applied field is assumed to be of the form $E\cos\omega t$.

The usual definition of the complex dielectric constant k is $k = \frac{D}{E} = 1 + 4\pi \frac{P}{E}$, where P is the polarization (dipole moment) per unit volume. Since the dipole moment per unit volume is given by the product of charge and displacement, the solution of (B-1) may be used to calculate the quadrature component of k. This, in turn, may be related to the absorption coefficient α. For a gas containing N particles per unit volume, $P = Ne\bar{x}$ where $\bar{x}$ is the average of the displacements of each individual charge from their equilibrium positions. The displacement x obtained from (B-1), when averaged over all molecules, yields the following form for $\bar{x}$,

$$\bar{x} = aE\cos\omega t + bE\sin\omega t \qquad \text{(B-2)}$$

Thus, the in-phase and quadrature-phase components of k are given by

$$k_i = 1 + 4\pi Nae \qquad \text{(B-3a)}$$

and

$$k_q = 4\pi Nbe \qquad \text{(B-3b)}$$

To determine the coefficients a and b in Equation (B-2), the general solution of (B-1) and the process of averaging must be examined in greater detail. For the sake of brevity, only the pertinent results will be discussed.

The solution of (B-1) is assumed to be of the form

$$x = \mathrm{Re}\left[\frac{eEe^{j\omega t}}{m(\omega_o^2 - \omega^2)} + C_1 e^{j\omega_o t} + C_2 e^{-j\omega_o t}\right]$$

where the coefficients C_1 and C_2 are functions of the time of occurrence of the last collision experienced by the molecule. Moreover, C_1 and C_2 depend on the initial values of x and $\dot{x}$. Thus, the evaluation of C_1 and C_2 requires an average taken over the distribution of collisions. The resulting value of b is found to be

$$b = \frac{\omega e}{2m\omega_o \tau}\left[\frac{1}{(\omega - \omega_o)^2 + \left(\frac{1}{\tau}\right)^2} + \frac{1}{(\omega + \omega_o)^2 + \left(\frac{1}{\tau}\right)^2}\right] \qquad \text{(B-4)}$$

where τ is the mean time between collisions.

Since the absorption coefficient α is merely the amount of radiation absorbed per unit length divided by the total radiation energy passing through a unit cube perpendicular to one of the faces, the following equation applies

$$\alpha = \frac{\frac{1}{4\pi}\left\langle E \cdot \frac{dp}{dt}\right\rangle_{av}}{\frac{cE^2}{8\pi}} = \frac{\frac{1}{4\pi}\left\langle E\cos t \quad \frac{d}{dt}(k_i E\cos t + k_q E\sin t)\right\rangle_{av}}{\frac{cE^2}{8\pi}}$$

$$= \frac{\omega k_q}{8\pi} \qquad \text{(B-5)}$$

where $\left\langle \quad \right\rangle_{av}$ denotes a time average over one cycle of the electromagnetic field and cgs units are assumed.

Hence, Equations (B-3b), (B-4) and (B-5) may be combined to yield

$$\alpha = \frac{2\pi N_e^2 \omega^2}{m\omega_o^2 \tau C} \left[\frac{1}{(\omega - \omega_o)^2 + \left(\frac{1}{\tau}\right)^2} + \frac{1}{(\omega + \omega_o)^2 + \left(\frac{1}{\tau}\right)^2} \right] \qquad \text{(B-6)}$$

$$= \frac{N_e^2 f^2}{mcf_o^2} \left[\frac{\frac{1}{2\pi\tau}}{(f - f_o)^2 + \left(\frac{1}{2\pi\tau}\right)^2} + \frac{\frac{1}{2\pi\tau}}{(f + f_o)^2 + \left(\frac{1}{2\pi\tau}\right)^2} \right]$$

To generalize (B-6) to the quantum mechanical case, it is found that $\frac{e^2}{m}$ must be replaced by $\frac{8\pi^2}{3h}|\mu_{ij}|^2 f_o$, where $|\mu_{ij}|$ is the effective dipole moment for a transition from an energy state i to another state j. Moreover, since the probability of a transition from the upper state to the lower one is the same as from the lower to the upper, the intensity is proportional to the difference in the population of the two states. If n is the number in the lower energy state, Boltzmann's distribution function requires that the number in the upper state be $ne^{-\frac{hf}{kT}}$, where hf is the difference in energy of the two levels and T is the absolute temperature. The difference in the population of the states is, therefore, $n(1 - e^{-\frac{hf}{kT}})$. Furthermore, the possibility of the existence of other allowable energy states necessitates the inclusion of another factor f_i, representing the fraction of the total number of

molecules that are in the lower of the two states of interest.

Consequently, the resulting expression for α is

$$\alpha = \frac{8\pi^2 N f_i |\mu_{ij}|^2 f^2}{3ckT\Delta f} \left[\frac{(\Delta f)^2}{(f - f_o)^2 + (\Delta f)^2} + \frac{(\Delta f)^2}{(f + f_o)^2 + (\Delta f)^2} \right]$$

$$= \alpha_o \left[\frac{(\Delta f)^2}{(f - f_o)^2 + (\Delta f)^2} + \frac{(\Delta f)^2}{(f + f_o)^2 + (\Delta f)^2} \right] \qquad \text{(B-7)}$$

where $\Delta f = \frac{1}{2\pi\tau}$ and it is assumed that $hf << kT$.

APPENDIX C

THE STARK EFFECT

The fundamental property of the Stark effect is that it changes the natural resonant frequencies of a system when the system is subjected to an applied electric field. In the case of molecules possessing a permanent dipole moment, the applied field exerts a torque upon the molecules thereby perturbing the total energy of the system. Although considerable discussion of the Stark effect may be found in the literature, a short review of the techniques for computing the magnitude of the change in energy levels, and hence transition frequencies, will be presented. Both symmetric-top and linear molecules will be considered.

In a typical case, the change in the energy levels produced by an applied field will be small compared to the total rotational energy. Therefore, standard perturbational techniques may be used to estimate the changes in the wave functions (eigenfunctions) and allowable energy states (eigenvalues) of a polarized rotating molecular top when an electric field is applied.

Assume, then, that the exact Hamiltonian of the perturbed system is given by

$$H = H^{(0)} + \lambda H^{(1)} \qquad \text{(C-1)}$$

where $H^{(0)}$ is a solution of the wave equation for the unperturbed system

$$H^{(0)}\psi_n^{(0)} = \varepsilon_n^{(0)}\psi^{(0)} \qquad \text{(C-2)}$$

with known eigenfunctions $\psi_n^{(0)}$ and eigenvalues $\varepsilon_n^{(0)}$, n being an index denoting a particular rotational state. In addition, the term $H^{(1)}$ is the perturbation term and λ is a constant ($0 \leq \lambda \leq 1$) which allows adjustment of the magnitude of the perturbation from zero to its full value.

We further assume that the eigenfunctions ψ_n and eigenvalues ε_n of the perturbed system may be represented as a power series in λ:

$$\psi_n = \psi_n^{(0)} + \lambda\psi_n^{(1)} + \lambda^2\psi_n^{(2)} + \cdots \qquad \text{(C-3)}$$

and

$$\varepsilon_n = \varepsilon_n^{(0)} + \lambda\varepsilon_n^{(1)} + \lambda^2\varepsilon_n^{(2)} + \cdots \qquad \text{(C-4)}$$

Thus, the true wave function of the perturbed system is found from

$$H\psi = \varepsilon\psi \qquad \text{(C-5)}$$

where only those solutions which obey

$$H\psi_n = \varepsilon_n\psi_n \qquad \text{(C-6)}$$

are possible eigenfunctions of real systems.

To find an approximate solution of (C-6), expressions (C-1), (C-3), and (C-4) may be inserted into (C-6). After rearranging terms according to powers of λ, we obtain

$$(H^{(0)}\psi_n^{(0)} - \varepsilon_n^{(0)}\psi_n^{(0)}) + \lambda(H^{(0)}\psi_n^{(1)} + H^{(1)}\psi_n^{(0)} - \varepsilon_n^{(0)}\psi_n^{(1)} - \varepsilon_n^{(1)}\psi_n^{(0)}) \tag{C-7}$$

$$+ \lambda^2(H^{(0)}\psi_n^{(2)} + H^{(1)}\psi_n^{(1)} - \varepsilon_n^{(0)}\psi_n^{(2)} - \varepsilon_n^{(1)}\psi_n^{(1)} - \varepsilon_n^{(2)}\psi_n^{(0)}) + \lambda^3(\cdots) = 0$$

This equation must hold for any arbitrary λ, hence, if the series is convergent, each of the coefficients of powers of λ must vanish separately. The zero order solution is obtained by setting the coefficient of λ^o to zero,

$$H^{(0)}\psi_n^{(0)} - \varepsilon_n^{(0)}\psi_n^{(0)} = 0$$

This is merely Equation (C-2) again.

The first order equation is

$$H^{(0)}\psi_n^{(1)} - \varepsilon_n^{(0)}\psi_n^{(1)} = (\varepsilon_n^{(1)} - H^{(1)})\psi_n^{(0)} \tag{C-8}$$

Furthermore, we may assume that $\psi_n^{(1)}$, $\psi_n^{(2)}$, etc. ..., can also be expressed in terms of the zero order wave functions $\psi_i^{(0)}$ since these form a complete set of orthonormal functions.

Letting

$$\psi_n^{(1)} = \sum_i a_i \psi_i^{(0)}$$

and substituting this into (C-8) we find

$$\sum_i a_i(\varepsilon_i^{(0)} - \varepsilon_n^{(0)})\psi_i^{(0)} = (\varepsilon_n^{(1)} - H^{(1)})\psi_n^{(0)} \qquad \text{(C-9)}$$

To obtain $\varepsilon_n^{(1)}$, the correction to the zero order energy required by the addition of the perturbation $H^{(1)}$ to the zero order Hamiltonian $H^{(0)}$, we multiply to the left, each side of (C-9), by $\psi_n^{(0)*}$ (the complex conjugate of $\psi_n^{(0)}$):

$$\sum_i a_i(\varepsilon_i^{(0)} - \varepsilon_n^{(0)})\psi_n^{(0)*}\psi_i^{(0)} = \varepsilon_n^{(1)}\psi_n^{(0)*}\psi_n^{(0)} - \psi_n^{(0)*}H^{(1)}\psi_n^{(0)} \qquad \text{(C-10)}$$

In (C-10), it is assumed that the a's and the ε's are constants and may be interchanged, in order, with $\psi_n^{(0)*}$. $H^{(1)}$, being an operator, however, cannot be interchanged with $\psi_n^{(0)*}$ in general. Next, each term in (C-10) is multiplied by the volume element $d\tau$ and integrated over the entire coordinate space τ,

$$\sum_i a_i(\varepsilon_i^{(0)} - \varepsilon_n^{(0)})\int_\tau \psi_n^{(0)*}\psi_i^{(0)}d\tau = \varepsilon_n^{(1)}\int_\tau \psi_n^{(0)*}\psi_n^{(0)}d\tau - \int_\tau \psi_n^{(0)*}H^{(1)}\psi_n^{(0)}d\tau \qquad \text{(C-11)}$$

Based on the orthonormality of the $\psi_i^{(0)}$, all of the terms on the left are zero. Hence,

$$\varepsilon_n^{(1)} = \int_\tau \psi_n^{(0)*} H^{(1)} \psi_n^{(0)} d\tau \qquad \text{(C-12)}$$

and the first order perturbation to the nth energy level may be readily found from the known zero order eigenfunctions $\psi_n^{(0)}$.

The coefficients a_i in the expression for the correction term $\psi_n^{(1)}$ may be obtained by multiplying, to the left, each side of (C-9) by $\psi_m^{(0)*}$ $(m \neq n)$ and subsequently integrating each term over the entire coordinate space as before,

$$\sum_i a_i(\varepsilon_i^{(0)} - \varepsilon_n^{(0)}) \int_\tau \psi_m^{(0)*} \psi_i^{(0)} d\tau = \varepsilon_n^{(1)} \int_\tau \psi_m^{(0)*} \psi_n^{(0)} d\tau - \int_\tau \psi_m^{(0)*} H^{(1)} \psi_n^{(0)} d\tau \qquad \text{(C-13)}$$

Again, the orthonormality of the eigenfunctions $\psi_i^{(0)}$ indicates that the only nonzero term on the left of (C-13) is that for i = m. Hence,

$$a_m(\varepsilon_m^{(0)} - \varepsilon_n^{(0)}) = -\int_\tau \psi_m^{(0)*} H^{(1)} \psi_n^{(0)} d\tau, \quad m \neq n$$

Solving for a_m, the coefficients of the terms in $\psi_n^{(1)}$ may be determined. Thus, the first order correction to $\psi_n^{(0)}$ is,

$$\psi_n^{(1)} = \sum_m \frac{-\int_\tau \psi_m^{(0)*} H^{(1)} \psi_n^{(0)} d\tau}{\varepsilon_m^{(0)} - \varepsilon_n^{(0)}} \psi_m^{(0)}, \quad m \neq n \qquad \text{(C-14)}$$

The second order equation is, from (C-7),

$$H^{(0)}\psi_n^{(2)} + H^{(1)}\psi_n^{(1)} - \varepsilon_n^{(0)}\psi_n^{(2)} - \varepsilon_n^{(1)}\psi_n^{(1)} - \varepsilon_n^{(2)}\psi_n^{(0)} = 0 \quad \text{(C-15)}$$

This time it is assumed that $\psi_n^{(2)}$ may be represented by

$$\psi_n^{(2)} = \sum_i b_i \psi_n^{(0)}$$

and that $\varepsilon_n^{(1)}$ and $\psi_n^{(1)}$ are given by (C-12) and (C-14), respectively. Therefore, we may rewrite (C-15) in the form

$$\sum_i b_i H^{(0)}\psi_i^{(0)} + \sum_m \frac{\left[-\int_\tau \psi_m^{(0)*} H^{(1)} \psi_n^{(0)} d\tau\right]}{\varepsilon_m^{(0)} - \varepsilon_n^{(0)}} H^{(1)}\psi_m^{(0)} - \varepsilon_n^{(0)} \sum_i b_i \psi_i^{(0)}$$

$$- \left[\int_\tau \psi_n^{(0)*} H^{(1)} \psi_n^{(0)} d\tau\right] \sum_m \frac{\left[-\int_\tau \psi_m^{(0)*} H^{(1)} \psi_n^{(0)} d\tau\right]}{\varepsilon_m^{(0)} - \varepsilon_n^{(0)}} \psi_m^{(0)}$$

$$- \varepsilon_n^{(0)}\psi_n^{(0)} = 0 \quad \text{(C-16)}$$

Since $H^{(0)}\psi_i^{(0)} = \varepsilon_i^{(0)}\psi_i^{(0)}$, the first term may be recast in the form $\sum_i b_i \varepsilon_i^{(0)}\psi_i^{(0)}$. Combining this with the third term, multiplying all terms by $\psi_n^{(0)*}$ and $d\tau$, and finally integrating over the coordinate space, one obtains:

$$\sum_i b_i(\varepsilon_i^{(0)} - \varepsilon_n^{(0)}) \int_\tau \psi_n^{(0)*}\psi_i^{(0)} d\tau + \sum_m \frac{\left[-\int_\tau \psi_m^{(0)*} H^{(1)} \psi_n^{(0)} d\tau\right]}{\varepsilon_m^{(0)} - \varepsilon_n^{(0)}} \int_\tau \psi_n^{(0)*} H^{(1)} \psi_m^{(0)} d\tau$$

$$- \int_\tau \psi_n^{(0)*} H^{(1)} \psi_n^{(0)} d\tau \sum_m \frac{\left[-\int_\tau \psi_m^{(0)*} H^{(1)} \psi_n^{(0)} d\tau\right]}{\varepsilon_m^{(0)} - \varepsilon_n^{(0)}} \int_\tau \psi_n^{(0)*} \psi_m^{(0)} d\tau$$

$$- \varepsilon_n^{(2)} \int_\tau \psi_n^{(0)*} \psi_n^{(0)} d\tau = 0 \qquad m \neq n \tag{C-17}$$

In (C-17), as a consequence of the orthonormality of the $\psi_n^{(0)}$'s, the first and third terms are identically zero while the coefficient of $\varepsilon_n^{(2)}$ is unity. Hence, the second order correction to the energy eigenvalue is

$$\varepsilon_n^{(2)} = \sum_m \frac{\left[\int_\tau \psi_m^{(0)*} H^{(1)} \psi_n^{(0)} d\tau\right]\left[\int_\tau \psi_n^{(0)*} H^{(1)} \psi_m^{(0)} d\tau\right]}{\varepsilon_n^{(0)} - \varepsilon_m^{(0)}}, \qquad m \neq n \tag{C-18}$$

Having obtained expressions for the correction terms which must be added to the energy eigenvalues of an unperturbed molecule when an electric field is applied, the change in transition frequencies may now be determined. Utilizing Equations (C-12) and (C-18) and the eigenfunctions obtained as shown in Appendix A, Gordy and his colleagues have shown that the correction terms for the (J,K,M) state due to the additional potential energy $-\mu E\cos\theta$ (θ is the angle between the direction of the dipole moment μ and the direction of the field E) are given by

$$\varepsilon_{JKM}^{(1)} = \frac{-\mu EKM}{J(J+1)} \tag{C-19}$$

and

$$\varepsilon_{JKM}^{(2)} = \frac{-(\mu E)^2}{2hB}\left[\frac{3M^2 - J(J+1)}{J(J+1)(2J-1)(2J+3)}\right] \tag{C-20}$$

In the preceding it is assumed that the dipole moment μ is in the direction of the axis of highest symmetry. Obviously, $\varepsilon_n^{(1)}$ is zero for symmetric top molecules with K = 0 and, hence, for all linear molecules. Thus, the need for computing the second order term is apparent. For $K \neq 0$, it may be demonstrated that the second order term is negligible with respect to the first order term. Therefore, only $\varepsilon_n^{(1)}$ need be calculated in determining the effect of perturbations to symmetric-top molecules for $K \neq 0$, while $\varepsilon_n^{(2)}$ is necessary for linear molecule calculations.

Consequently, the transition frequencies for a symmetric-top molecule (K = 0), in the presence of an applied field E, are

$$f_o = \frac{\varepsilon_{J+1,K,M}^{(0)} + \varepsilon_{J+1,K,M}^{(1)} - \varepsilon_{JKM}^{(0)} - \varepsilon_{JKM}^{(1)}}{h} \tag{C-21}$$

$$= 2B(J+1) + 2\left(\frac{\mu E}{h}\right)\frac{MK}{J(J+1)(J+2)} \tag{C-21}$$

where B is a molecular constant (described in Appendix A).

For a linear molecule, or symmetric-top molecule with K = 0, the

corresponding expression is

$$f_o = \frac{\varepsilon^{(0)}_{J+1,M} + \varepsilon^{(2)}_{J+1,M} - \varepsilon^{(0)}_{JM} - \varepsilon^{(2)}_{JM}}{h} \qquad \text{(C-22)}$$

$$= 2B(J+1) + \frac{(\mu E)^2}{(J+1)Bh^2} \frac{3M^2(8J^2 + 16J + 5) - 4J(J+1)^2(J+2)}{J(J+2)(2J-1)(2J+2)(2J+3)(2J+5)}$$

Hence, the shift in the resonant frequencies of symmetric-top and linear molecules when a Stark field E is applied, may be predicted by (C-21) and (C-22).

APPENDIX D

A PERTURBATIONAL FORMULA FOR PREDICTING THE CHANGE IN PROPAGATION FACTOR DUE TO THE TEFLON STARK ELECTRODE SUPPORTS

An estimate of the loss introduced by the presence of the Teflon strips used to support the Stark electrode may be obtained from a formula based on perturbational techniques.

Consider a rectangular waveguide which is filled with a medium having constitutive parameters ε_o and μ_o. If a portion of the medium within the waveguide is then replaced with a new material having parameters ε and μ, as shown in Figure D-1, the propagation factor for the perturbed waveguide will differ from that of the original waveguide.

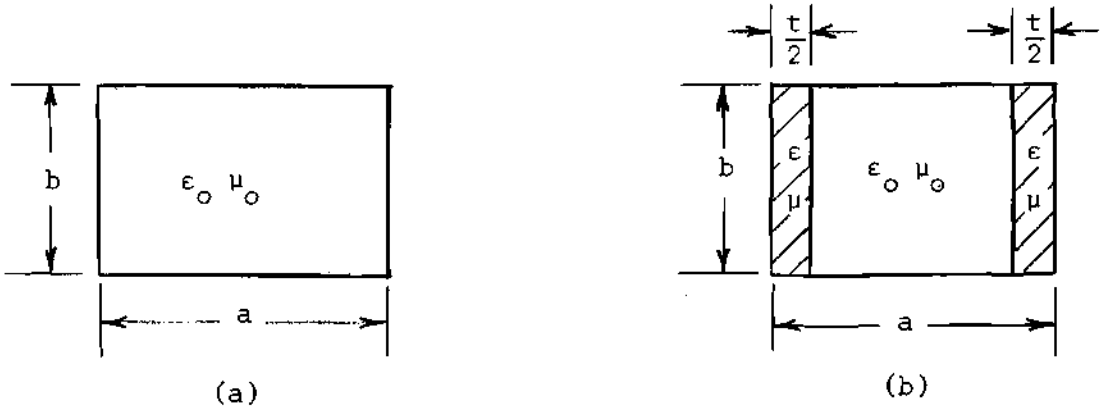

Figure D-1. Waveguide Cross-Sections:
(a) Unperturbed
(b) Perturbed

In the following paragraphs, a procedure will be described which yields an exact expression for the change in the propagation factor in such a situation. Utilizing certain simplifying assumptions, the exact formula may be modified to obtain a reasonable estimate of the true change.

It is assumed that the fields in the unperturbed waveguide are given by

$$\bar{E}_o = \hat{E}_o(x,y)e^{-j\beta_o z} \tag{D-1a}$$

and

$$\bar{H}_o = \hat{H}_o(x,y)e^{-j\beta_o z} \tag{D-1b}$$

while the actual fields in the perturbed waveguide are represented by

$$\bar{E} = \hat{E}(x,y)e^{-j\beta z} \tag{D-2a}$$

and

$$\bar{H} = \hat{H}(x,y)e^{-j\beta z} \tag{D-2b}$$

Maxwell's equations then require that

$$\nabla \times \bar{E}_o = -j\omega\mu_o\bar{H}_o \tag{D-3a}$$

$$\nabla \times \bar{H}_o = j\omega\epsilon_o\bar{E}_o \tag{D-3b}$$

$$\nabla \times \bar{E} = -j\omega\mu_1\bar{H} \tag{D-3c}$$

and

$$\nabla \times \bar{H} = j\omega\epsilon_1 \bar{E} \qquad \text{(D-3d)}$$

where μ_1 and ϵ_1 assume values appropriate to the region of interest. Then, scalarly multiply (D-3d) by the conjugate of $\bar{E}_o$ and the conjugate of (D-3a) by $\bar{H}$. The resulting two equations are

$$\bar{E}_o^* \cdot \nabla \times \bar{H} = j\omega\epsilon_1 \bar{E}_o^* \cdot \bar{E}$$

and

$$\bar{H} \cdot \nabla \times \bar{E}_o^* = j\omega\mu_o \bar{H} \cdot \bar{H}_o^*$$

Subtracting these and applying the identity

$$\nabla \cdot \bar{A} \times \bar{B} = \bar{B} \cdot \nabla \times \bar{A} - \bar{A} \cdot \nabla \times \bar{B}$$

results in the expression

$$\nabla \cdot \bar{H} \times \bar{E}_o^* = j\omega\epsilon_1 \bar{E}_o^* \cdot \bar{E} - j\omega\mu_o \bar{H} \cdot \bar{H}_o^* \qquad \text{(D-4)}$$

Analogous operations on (D-3b) and (D-3c) yield

$$\nabla \cdot \bar{H}_o^* \times \bar{E} = -j\omega\epsilon_o \bar{E} \cdot \bar{E}_o^* + j\omega\mu_1 \bar{H} \cdot \bar{H}_o^* \qquad \text{(D-5)}$$

The sum of (D-4) and (D-5) is

$$\nabla \cdot (\bar{H} \times \bar{E}_o^*) + \nabla \cdot (\bar{H}_o^* \times \bar{E}) = j\omega(\varepsilon_1 - \varepsilon_o)\bar{E} \cdot \bar{E}_o^* - j\omega(\mu_1 - \mu_o)\bar{H} \cdot \bar{H}_o^* \qquad \text{(D-6)}$$

Both sides of (D-6) may now be integrated over a volume τ of waveguide of infinitesimal length dz, and the identity $\iiint \nabla \cdot \bar{A} d\tau = \oiint \bar{A} \cdot ds$ applied to obtain

$$\iiint_\tau \left[\nabla \cdot (\bar{H} \times \bar{E}_o^*) + \nabla \cdot (\bar{H}_o^* \times \bar{E})\right] d\tau = \oiint_S (\bar{H} \times \bar{E}_o^* + \bar{H}_o^* \times \bar{E}) \cdot \bar{n}\, ds \qquad \text{(D-7)}$$

where S is the surface which bounds the volume τ and $\bar{n}$ is a unit vector normal to S. It is evident from (D-6) however, that the only portion of the volume which will contribute to the left side of (D-7) is that for which $\mu_1 - \mu_0$ and $\varepsilon_1 - \varepsilon_o$ are not both identically zero. Thus,

$$\iiint_\tau \left[\nabla \cdot (\bar{H} \times \bar{E}_o^*) + \nabla \cdot \bar{H}_o^* \times \bar{E}\right] d\tau = \qquad \text{(D-8)}$$

$$j\omega(\varepsilon - \varepsilon_o) \iiint_{\tau'} \bar{E} \cdot \bar{E}_o^* d\tau - j\omega(\mu - \mu_o) \iiint_{\tau'} \bar{H} \cdot \bar{H}_o^* d\tau$$

where τ' represents the volume occupied by the perturbing material. The surface integral on the right of (D-7) must be taken over the walls of the guide of length dz and over two cross-sections of guide separated by the infinitesimal distance dz. Since the components of $\bar{E}_o$ and $\bar{E}$ tangent to the waveguide walls must be identically zero, the surface

integral over the walls must be zero. Hence, the right side of (D-7) is given by

$$\oiint_S (\bar{H} \times \bar{E}_o^* + \bar{H}_o^* \times \bar{E}) \cdot \bar{n}\, ds = \tag{D-9}$$

$$\iint_{S_1} (\bar{H} \times \bar{E}_o^* + \bar{H}_o^* \times \bar{E}) \cdot \bar{n}_1 ds + \iint_{S_2} (\bar{H} \times \bar{E}_o^* + \bar{H}_o^* \times \bar{E}) \cdot \bar{n}_2 ds$$

where S_1 is a cross-section of the waveguide at one position and S_2 is a cross-section located dz units down the waveguide. In addition, $\bar{n}_1$ and $\bar{n}_2$ are unit normal vectors directed out of the volume formed by S_1, S_2 and the walls of the guide. Thus, $\bar{n}_1$ and $\bar{n}_2$ are equal in magnitude but point in opposite directions. Also, since the thickness of the volume is infinitesimal, one may assume

$$\iint_{S_2} = \iint_{S_1} + \left(\frac{\partial}{\partial z} \iint_{S'}\right) dz$$

where S' is a surface between S_1 and S_2. Hence we obtain

$$\oiint_S (\bar{H} \times \bar{E}_o^* + \bar{H}_o^* \times \bar{E}) \cdot \bar{n} ds = \frac{\partial}{\partial z} \iint_{S'} (\bar{H} \times \bar{E}_o^* + \bar{H}_o^* \times \bar{E}) \cdot \bar{n}_2 ds \tag{D-10}$$

Now, the fields given by (D-1) and (D-2) may be inserted into the right-hand member of (D-10). The result of this manipulation is

$$\oint\!\!\!\!\!\!\int_S (\bar{H} \times \bar{E}_o^* + \bar{H}_o^* \times \bar{E}) \cdot \bar{n} ds = \tag{D-11}$$

$$-j(\beta - \beta_o) e^{-j(\beta-\beta_o)z} dz \iint_{S'} (\hat{H} \times \hat{E}_o^* + \hat{H}_o^* \times \hat{E}) \cdot \bar{n}_2 ds$$

Thus from (D-7), (D-8), and (D-11) we find

$$j\omega(\varepsilon - \varepsilon_o) \iiint_{\tau'} \bar{E} \cdot \bar{E}_o^* d\tau - j\omega(\mu - \mu_o) \iiint_{\tau'} \bar{H} \cdot \bar{H}_o^* d\tau = \tag{D-12}$$

$$-j(\beta - \beta_o) e^{-j(\beta-\beta_o)z} dz \iint_{S'} (\hat{H} \times \hat{E}_o^* + \hat{H}_o^* \times \hat{E}) \cdot \bar{n}_2 ds$$

Also, $\bar{E} \cdot \bar{E}_o^*$ and $\bar{H} \cdot \bar{H}_o^*$ may be expressed in terms of $\hat{E} \cdot \hat{E}_o^*$ and $\hat{H} \cdot \hat{H}_o^*$, respectively. Then, the left side of (D-12) may be rewritten as

$$j\omega(\varepsilon - \varepsilon_o) \iiint_{\tau'} \bar{E} \cdot \bar{E}_o^* d\tau - j\omega(\mu - \mu_o) \iiint_{\tau'} \bar{H} \cdot \bar{H}_o^* d\tau = \tag{D-13}$$

$$j\omega(\varepsilon - \varepsilon_o) e^{-j(\beta-\beta_o)z} \iiint_{\tau'} \hat{E} \cdot \hat{E}_o^* d\tau - j\omega(\mu - \mu_o) e^{-j(\beta-\beta_o)z} \iiint_{\tau'} \hat{H} \cdot \hat{H}_o^* d\tau$$

Finally, it is assumed that

$$\iiint_{\tau'} (\cdot) d\tau = dz \iint_{S''} (\cdot) ds \ ,$$

where S" is the cross-section of the perturbing material. Combining (D-12) and (D-13) yields the desired expression:

$$\beta - \beta_o = - \frac{\omega(\varepsilon - \varepsilon_o) \iint_{S''} \hat{E} \cdot \hat{E}_o^* ds - \omega(\mu - \mu_o) \iint_{S''} \hat{H} \cdot \hat{H}_o^* ds}{\iint_{S'} (\hat{H} \times \hat{E}_o^* + \hat{H}_o^* \times \hat{E}) \cdot \bar{n}_2 ds} \qquad \text{(D-14)}$$

Equation (D-14) is an exact expression for the change in the propagation factor in terms of the true fields before and after the perturbation and of the parameters of the perturbing material.

In the case of interest it will be assumed that $\mu = \mu_o$, $\varepsilon = \varepsilon_1 \cdot (1 - j\tan\delta)$, and that the fields $\hat{E}$, $\hat{H}$ in the perturbed waveguide are identical in form to the dominant mode in the unperturbed waveguide. Also, since the dominant mode is symmetric with respect to a plane normal to the broad walls and located midway between the narrow walls, the integrals in the numerator of (D-14) need be evaluated only over the cross-section of one of the Teflon strips and the result subsequently doubled. The resulting expression is

$$\beta - \beta_o = \frac{-2\omega(\varepsilon_1 - \varepsilon_o - j\varepsilon_1\tan\delta) \int_0^{\frac{t}{2}} \int_0^b |\hat{E}_o|^2 dy dx}{\int_0^a \int_0^b (\hat{H}_o \times \hat{E}_o^* + \hat{H}_o^* \times \hat{E}_o) \cdot \bar{n}_2 dy dx} \qquad \text{(D-15)}$$

$$= \frac{-2\omega(\varepsilon_1 - \varepsilon_o - j\varepsilon_1\tan\delta) b C^2 \int_0^{\frac{t}{2}} \sin^2 \frac{\pi x}{a} dx}{-2 \frac{C^2}{Z_{TE_{10}}} b \int_0^a \sin^2 \frac{\pi x}{a} dx}$$

$$= \omega(\varepsilon_1 - \varepsilon_o - j\varepsilon_1 \tan\delta)\left(\frac{t}{2a} - \frac{1}{2\pi}\sin\frac{\pi t}{a}\right)Z_{TE_{10}}$$

In the oversized waveguide absorption cell $\lambda \approx \lambda_{\text{free space}}$. Thus $Z_{TE} \approx \sqrt{\mu_o/\varepsilon_o} = \beta_o/\omega\varepsilon_o$ and Equation (D-15) may be recast as

$$\beta - \beta_o = \beta_o\left(\frac{\varepsilon_1 - \varepsilon_o}{\varepsilon_o} - j\,\frac{\varepsilon_1}{\varepsilon_o}\tan\delta\right)\left(\frac{t}{2a} - \frac{1}{2\pi}\sin\frac{\pi t}{a}\right) \qquad \text{(D-16)}$$

Finally, for $\frac{t}{2a} << 1$, the term $\left(\frac{t}{2a} - \frac{1}{2\pi}\sin\frac{\pi t}{a}\right)$ is very nearly $\frac{\pi^2}{12}\left(\frac{t}{a}\right)^3$. In this case, the change in propagation factor due to the thin dielectric slabs along each sidewall of the waveguide is approximated by

$$\beta - \beta_o = \beta_o\,\frac{\pi^2}{12}\left(\frac{t}{a}\right)^3\left(\frac{\varepsilon_1 - \varepsilon_o}{\varepsilon_o} - j\,\frac{\varepsilon_1}{\varepsilon_o}\tan\delta\right) \qquad \text{(D-17)}$$

This expression may then be utilized to predict both the change in the velocity of propagation and the appearance of an attenuation factor due to a lossy dielectric characterized by ε_1 and $\tan\delta$.

LITERATURE CITED

1. C. E. Cleeton and N. H. Williams, "Electromagnetic Waves of 1.1 Cm Wavelength and the Absorption Spectrum of Ammonia," Phys. Rev., vol. 45, p. 391, Feb. 15, 1934.

2. F. Reiche and H. Rademacher, "Die Quantelung des symmetrischen Kreisels nach Schrödingers Undulationsmechanik," Zeit. für Phys., vol. 39, 1927.

3. E. Schrödinger, "Über das Verhältnis der Heisenberg-Born-Jordanschen Quantenmechanik zu der meinen," Ann. der Phys., vol. 79, 1926.

4. H. Nielson, "The Vibration-Rotation Energies of Molecules," Revs. Mod. Phys., vol. 23, p. 90, 1951.

5. W. Gordy, W. V. Smith, and R. F. Trambarulo, *MICROWAVE SPECTROSCOPY*, New York: Dover, 1966, p. 103.

6. J. H. Van Vleck and V. F. Weisskopf," On the Shape of Collision Broadened Lines," Rev. Mod. Phys., vol. 17, p. 227, 1945.

7. Gordy et al., op. cit., p. 182.

8. C. H. Townes and A. L. Schawlow, *MICROWAVE SPECTROSCOPY*, New York: McGraw-Hill, 1955, p. 337.

9. Ibid., p. 375.

10. W. Gordy et al., op. cit., p. 156.

11. E. W. Fletcher and S. P. Cooke, Cruft Lab. ONR Report 64, May, 1950.

12. W. D. Hershberger and L. E. Norton," Frequency Stabilization with Microwave Spectral Lines," RCA Review, vol. 9, p. 38, 1948.

13. D. K. Cheng, *ANALYSIS OF LINEAR SYSTEMS*, Reading, Mass.: Addison-Wesley, 1959, p. 205.

14. C. H. Townes and A. L. Schawlow, op. cit., p. 371.

15. H. Häggblom, "The Spectral Density of the A. M. Noise in Reflex Klystrons," Proc. IEE, vol. 106, pt. B, No. 30, p. 18, Nov. 1959.

16. A. H. Uhlir. "Characterization of Crystal Diodes for Low-Level Microwave Detection," Microwave Journal, vol. VI, No. 7, p. 59, July, 1963.

17. B. G. Whitford, "The Video Resistance Concept in Nonlinear AM Detectors," The Microwave Journal, vol. VII, No. 4, p. 54, April, 1964.

18. C. M. Johnson, R. Trambarulo and W. Gordy, "Microwave Spectroscopy in the Region from Two to Three Millimeters, Part III," Phys. Rev., Vol. 84, No. 6, p. 1178, Dec. 15, 1951.

19. C. H. Townes and A. L. Schawlow, op. cit., p. 73.

20. Ibid., Appendix VI, p. 613.

21. E. C. Jordan, *ELECTROMAGNETIC WAVES AND RADIATING SYSTEMS*, Englewood Cliffs, N. J.: Prentice-Hall, 1950, p. 287.

22. R. F. Harrington, *TIME HARMONIC ELECTROMAGNETIC FIELDS*, New York: McGraw-Hill, 1961, p. 326.

23. K. H. Breeden and A. P. Sheppard, "Millimeter and Submillimeter Wave Dielectric Measurements with an Interference Spectrometer," Tech. Rept No. 1, Proj. A-934, Engineering Experiment Station, Georgia Institute of Technology, Atlanta, Ga., Nov. 17, 1966, pp. 13, 18.

24. P. Kisliuk and C. H. Townes, "Molecular Microwave Spectra Tables," NBS Circular 518, U. S. Dept. of Com., NBS, June 23, 1952.

25. P. Debye, *POLAR MOLECULES*, Chemical Catalog Company, Inc.: New York, 1929, Chapt. 5.

26. C. H. Townes and A. L. Schawlow, op. cit., p. 336.

VITA

Milton Edward Cram was born on July 16, 1939, in Wyandotte, Michigan, the son of Ernest M. and Lydia G. Cram. He was married in 1961 to Miss Linda Fox Henderson, and they have three children.

He attended public schools in Dearborn, Michigan, and graduated from Edsel B. Ford High School in June, 1957. He entered the Georgia Institute of Technology as a co-op student in June, 1957. He was employed as a co-op trainee in the Process Development Department of the Ford Motor Company from September, 1957, until June, 1961.

He received the BEE (Co-operative Plan) degree from the Georgia Institute of Technology in June, 1962.

He was employed as a Microwave Engineer with the Research Laboratories Division of the Bendix Corporation from 1962 to 1963.

Mr. Cram started his employment at the Georgia Institute of Technology in 1963 as a Research Assistant in the Communications Branch of the Engineering Experiment Station. From 1964 to 1966 he held a National Science Foundation Co-op Graduate Fellowship. During his fellowship activities he was employed as a Graduate Research Assistant in the School of Electrical Engineering.

Since June, 1966, he has been employed as an engineer with Scientific-Atlanta, Inc.